AMERICAN SOCIETY FOR MICROBIOLOGY | Journal of Bacteriology®

RESEARCH ARTICLE

RefZ and Noc Act Synthetically to Prevent Aberrant Divisions during *Bacillus subtilis* Sporulation

Allyssa K. Miller,[a] Jennifer K. Herman[a]

[a]Department of Biochemistry and Biophysics, Texas A&M University, College Station, Texas, USA

ABSTRACT During sporulation, *Bacillus subtilis* undergoes an atypical cell division that requires overriding mechanisms that protect chromosomes from damage and ensure inheritance by daughter cells. Instead of assembling between segregated chromosomes at midcell, the FtsZ-ring coalesces polarly, directing division over one chromosome. The DNA-binding protein RefZ facilitates the timely assembly of polar Z-rings and partially defines the region of chromosome initially captured in the forespore. RefZ binds to motifs (*RBM*s) located proximal to the origin of replication (*oriC*). Although *refZ* and the *RBM*s are conserved across the *Bacillus* genus, a *refZ* deletion mutant sporulates with wild-type efficiency, so the functional significance of RefZ during sporulation remains unclear. To further investigate RefZ function, we performed a candidate-based screen for synthetic sporulation defects by combining Δ*refZ* with deletions of genes previously implicated in FtsZ regulation and/or chromosome capture. Combining Δ*refZ* with deletions of *ezrA*, *sepF*, *parA*, or *minD* did not detectably affect sporulation. In contrast, a Δ*refZ* Δ*noc* mutant exhibited a sporulation defect, revealing a genetic interaction between RefZ and Noc. Using reporters of sporulation progression, we determined the Δ*refZ* Δ*noc* mutant exhibited sporulation delays after Spo0A activation but prior to late sporulation, with a subset of cells failing to divide polarly or activate the first forespore-specific sigma factor, SigF. The Δ*refZ* Δ*noc* mutant also exhibited extensive dysregulation of cell division, producing cells with extra, misplaced, or otherwise aberrant septa. Our results reveal a previously unknown epistatic relationship that suggests *refZ* and *noc* contribute synthetically to regulating cell division and supporting spore development.

IMPORTANCE The DNA-binding protein RefZ and its binding sites (*RBM*s) are conserved in sequence and location on the chromosome across the *Bacillus* genus and contribute to the timing of polar FtsZ-ring assembly during sporulation. Only a small number of noncoding and nonregulatory DNA motifs are known to be conserved in chromosomal position in bacteria, suggesting there is strong selective pressure for their maintenance; however, a *refZ* deletion mutant sporulates efficiently, providing no clues as to their functional significance. Here, we find that in the absence of the nucleoid occlusion factor Noc, deletion of *refZ* results in a sporulation defect characterized by developmental delays and aberrant divisions.

KEYWORDS FtsZ, Noc, RefZ, cell division, nucleoid occlusion, sporulation

Chromosome inheritance depends on precise division site selection. Abnormal divisions can result in aneuploidy, including total chromosome loss. Eukaryotes employ cell cycle checkpoints to ensure replication and segregation are complete before cytokinesis initiates. In contrast, bacteria often segregate DNA concurrently with division, so mechanisms to coordinate these processes are critical. To ensure faithful transmission of genetic material to progeny, bacteria segregate replicated DNA to opposite cell halves and divide between chromosome masses (nucleoids). Division at midcell is initiated by polymerization and bundling of membrane-tethered FtsZ

Editor Elizabeth A. Shank, University of Massachusetts Medical School

Address correspondence to Jennifer K. Herman, jkherman@tamu.edu.

The authors declare no conflict of interest.

Received 13 January 2022
Accepted 11 April 2022
Published 4 May 2022

protofilaments into the "Z-ring," a dynamic structure subject to both positive and negative regulation (1–20). The Z-ring facilitates recruitment of additional factors needed for division at midcell, including peptidoglycan remodeling enzymes (2, 14–20).

The Min system and Nucleoid Occlusion (NO) are redundant, but mechanistically distinct systems for ensuring Z-rings assemble at midcell, between chromosomes (21, 22). In *B. subtilis*, the MinCD complex localizes in the immediate vicinity of the nascent septum and inhibits additional Z-rings from forming (23–26); following division, Min inhibition persists at the newly formed, nucleoid-free poles (27, 28). NO, by contrast, prevents assembly of division-competent Z-rings over the bulk of the nucleoid (29, 30). In *E. coli*, NO is mediated by an inhibitor of FtsZ polymerization, SlmA. SlmA is also a DNA-binding protein, with specificity for motifs (SBSs) enriched throughout the chromosome except in the terminus (*ter*) region (30, 31). Following chromosome replication and segregation, *ter* is localized at midcell. The coincident segregation of SlmA away from midcell leads to release of NO, a condition more favorable to, but not sufficient for, Z-ring assembly. The NO protein of *B. subtilis*, Noc, also binds to motifs enriched distal to *ter* (32); however, unlike SlmA, Noc has not been shown to interact with FtsZ directly. Instead, Noc is hypothesized to block Z-ring nucleation sites by tethering the chromosome to the membrane (33). More recent, high resolution microscopy experiments suggest that rather than inhibiting Z-ring formation over the nucleoid, Noc promotes shifting of nonmedial Z-ring intermediates toward midcell in a process described as "corralling" (34). Notably, neither Min nor NO are required for midcell localization of FtsZ, though each contributes to the efficiency of medial division (21).

Division in bacteria is not always medial nor occluded by the presence of nucleoid. For example, the earliest stage of *B. subtilis* sporulation is characterized by an asymmetric septation over one chromosome, resulting in two cell compartments with transiently different genetic complements (35). The larger "mother" cell contains a complete copy of the chromosome, while the smaller future spore (forespore) initially captures only a segment of the origin-proximal region of a second chromosome (36–38); bisection of the forespore-destined chromosome is avoided because the DNA is threaded through the FtsK-like ATPase, SpoIIIE, which pumps the remainder of the chromosome into the forespore (39–41). The polar division of sporulation is of considerable interest because it requires bypass of the Min and NO systems active during vegetative growth (40, 42, 43). The redistribution of FtsZ from midcell to the pole is known to be facilitated by enhanced transcription of *ftsAZ* from a SigH-dependent promoter (P2) (44) and by expression of the FtsZ-associated protein SpoIIE (45). Remarkably, increasing *ftsAZ* copy number and artificially inducing *spoIIE* is sufficient to shift the Z-rings of nonsporulating cells toward the poles (46).

RefZ (Regulator of FtsZ) is a DNA-binding protein expressed by Spo0A-P during the early stages of sporulation (47). *refZ* is also repressed by the glucose repressor CcpA (48), activated under conditions of phosphate limitation (49), and is upregulated in stationary phase by SigH (50). During sporulation, RefZ binds to DNA motifs (*RBM*s) located near *oriC* (RBM_O) and on the left and right chromosomal arms (RBM_{L1}, RBM_{L2}, RBM_{R1}, and RBM_{R2}) (51, 52). The left and right arm *RBM*s fall at the boundary demarcating the segment of chromosome localized in the forespore at the time of polar septation (51). Cells lacking *refZ* or the *RBM*s are more likely to capture DNA regions generally excluded from the forespore at the time of polar division, indicating that RefZ-*RBM* complexes somehow influence the position of the septum relative to the chromosome (51). During sporulation, a Δ*refZ* mutant also exhibits, on average, a delay in polar Z-ring formation (52) and a small shift of the septum toward midcell (53). These results suggest the Δ*refZ* mutant's "overcapture" phenotype may be at least partially attributable to changes in chromosome organization or increased forespore dimensions that arise due to the delay.

There is likely a strong selective advantage to maintaining *RBM* positioning on the chromosome, as the arrangement of the *RBM*s on the left and right chromosome arms is remarkably conserved across the entire *Bacillus* genus (51); however, deleting *refZ* or introducing mutations into the *RBM*s that prevent RefZ binding does not reduce sporulation efficiency under standard laboratory growth conditions (51, 54). The mechanism

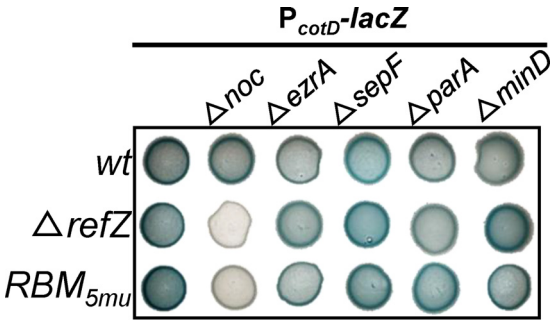

FIG 1 Plate-based sporulation assay based on *lacZ* expression from a late-stage sporulation promoter, P$_{cotD}$. *wt* (BAM1323), Δ*noc* (BAM1321), Δ*ezrA* (BAM1563), Δ*sepF* (BAM1548), Δ*parA* (BAM1549), Δ*minD* (BAM1575), Δ*refZ* (BAM1550), Δ*refZ* Δ*noc* (BAM1546), Δ*refZ* Δ*ezrA* (BAM1559), Δ*refZ* Δ*sepF* (BAM1577), Δ*refZ* Δ*parA* (BAM1568), Δ*refZ* Δ*minD* (BAM1578), *RBM*$_{5mu}$ (BAM1573), *RBM*$_{5mu}$ Δ*noc* (BAM1562), *RBM*$_{5mu}$ Δ*ezrA* (BAM1564), *RBM*$_{5mu}$ Δ*sepF* (BAM1547), *RBM*$_{5mu}$ Δ*parA* (BAM1569), *RBM*$_{5mu}$ Δ*minD* (BAM1576).

underlying RefZ's observed effects on FtsZ, and the selective advantage conferred to *Bacillus* by maintaining *refZ* and the *RBM*s are not known.

In this work, we performed a candidate-based screen to determine if deleting *refZ* in combination with other genes previously implicated in FtsZ regulation and/or chromosome capture would result in synthetic sporulation phenotypes. We found that combining Δ*refZ* with deletions of *ezrA*, *sepF*, *parA*, or *minD* did not detectably reduce sporulation efficiency. In contrast, reduced sporulation of a Δ*refZ* Δ*noc* mutant was evident in a plate-based assay. Using reporters of sporulation progression, we determined that the sporulation defect occurred after Spo0A activation, but prior to late sporulation. A subpopulation of Δ*refZ* Δ*noc* mutant cells failed to divide polarly or, following division, to activate the first forespore sigma factor. In addition, the Δ*refZ* Δ*noc* mutant exhibited aberrant divisions indicative of dysregulated Z-ring assembly. Our results reveal an epistatic relationship between RefZ and Noc consistent with the two proteins contributing synthetically to cell division regulation and spore development.

RESULTS

Deletion of *refZ* and *noc* results in a synthetic sporulation defect. RefZ promotes shifting of medial Z-rings toward the pole and the precise capture of chromosome in the forespore, yet deletion of *refZ* does not affect sporulation efficiency (51, 52), suggesting RefZ function is redundant with other factors affecting cell division and/or chromosome capture. To look for synthetic sporulation defects, we integrated a reporter of late-stage sporulation, P$_{cotD}$-*lacZ*, into the chromosome at an ectopic locus. In this background, cells reaching late-stage sporulation express beta-galactosidase, resulting in accumulation of blue pigment on sporulation medium containing X-gal (Fig. 1). When spotted at equivalent densities, Δ*refZ* cells turned blue at a rate indistinguishable from wild type (Fig. 1), consistent with prior results demonstrating that the Δ*refZ* mutant does not exhibit a sporulation defect (51, 52). A mutant harboring point mutations that abrogate RefZ binding at the five origin-proximal *RBM*s (51), *RBM*$_{5mu}$, also sporulated indistinguishably from wild type in the plate-based assay (Fig. 1).

Next, we assessed expression of P$_{cotD}$-*lacZ* in strains harboring deletions of genes implicated in regulating FtsZ dynamics (*noc*, *ezrA*, and *sepF*) (7, 32, 43, 55, 56), chromosome capture (*soj*) (56–58), or both (*minD*) (55, 56). Again, each of the single deletion strains progressed in sporulation comparably to wild type (Fig. 1). Similar results were obtained when each deletion was introduced into a Δ*refZ* or *RBM*$_{5mu}$ mutant background, with two exceptions: the Δ*refZ* Δ*noc* and *RBM*$_{5mu}$ Δ*noc* mutants did not turn blue during the experimental time course (Fig. 1), consistent with a defect or halt in sporulation progression.

To determine if the mutants produced viable spores, we grew cells in a sporulation medium and determined the number of CFU before and after a heat treatment that

TABLE 1 Sporulation efficiencies of wild type and mutants[a]

Genotype	CFU/mL	Spores/mL	% spores/CFU	% spores/wt spores
wt	2.3×10^8 ($\pm$ 5.7×10^7)	2.7×10^8 ($\pm$ 5.4×10^7)	124 ($\pm$ 26)	100
Δ*refZ*	2.2×10^8 ($\pm$ 3.5×10^7)	2.1×10^8 ($\pm$ 2.9×10^7)	90 ($\pm$ 25)	77 ($\pm$ 12)
RBM_{5mu}	3.4×10^8 ($\pm$ 3.8×10^7)	1.9×10^8 ($\pm$ 3.9×10^7)	57 ($\pm$ 19)	70 ($\pm$ 14)
Δ*noc*	2.1×10^8 ($\pm$ 2.8×10^7)	1.4×10^8 ($\pm$ 2.2×10^7)	69 ($\pm$ 11)	55 ($\pm$ 12)
Δ*refZ* Δ*noc*	7.0×10^7 ($\pm$ 5.4×10^6)	5.2×10^7 ($\pm$ 4.7×10^5)	74 ($\pm$ 6)	20 ($\pm$ 4)
RBM_{5mu} Δ*noc*	9.1×10^7 ($\pm$ 8.5×10^6)	3.3×10^7 ($\pm$ 3.8×10^6)	36 ($\pm$ 1)	12 ($\pm$ 2)

[a]Values shown are the average of three experimental and biological replications, with standard deviations in parentheses.

kills vegetative cells. The single mutants produced spores at levels within 2-fold of wild-type, consistent with either no or a minor sporulation defect (Table 1). In contrast, the double mutants produced 5–10-fold fewer spores. Notably, the double mutants also exhibited around a 2-fold drop in CFU before heat treatment, suggesting that a subset of cells committed to sporulation (59), but were unable to complete the sporulation process. We conclude that RefZ and the *RBM*s contribute synthetically with Noc to support wild-type sporulation.

Δ*refZ* Δ*noc and* RBM_{5mu} Δ*noc* mutants initiate sporulation. The sporulation delay observed in the Δ*refZ* Δ*noc* and RBM_{5mu} Δ*noc* double mutants could be due to failed or reduced entry into the sporulation program or to a delay or halt at any stage of sporulation prior to *cotD* expression. To investigate further, we introduced a fluorescent reporter (P_{spoIIG}-*CFP*) activated during the earliest stage of sporulation by the sporulation master regulator, Spo0A-P (48, 60). Using P_{spoIIG}-*CFP*, we were able to identify cells that had initiated sporulation, including cells without polar septa. Two and a half hours after resuspension in sporulation medium, cells were collected, and CFP expression was monitored by epifluorescence microscopy. The single and double mutants were qualitatively indistinguishable from wild type with respect to the number of CFP-expressing cells (Fig. 2 and Fig. S1), suggesting that the sporulation defect in Δ*refZ* Δ*noc* and RBM_{5mu} Δ*noc* mutant cells occurs after sporulation is initiated; however, we do not exclude the possibility that a subset of cells may also fail to initiate.

While the double mutants displayed no qualitative delay in Spo0A-P activation, it was evident that the frequency of cells expressing CFP but lacking polar septa was increased (Fig. 2 and Fig. S1). To quantitate, the CFP channels of all images were scaled identically, and cells lacking polar septa were scored as either expressing CFP or not (Fig. 3 and Table 2). Notably, while only 5–12% of aseptate cells expressed CFP in wild type and the single mutants, this value increased to 36% and 54% in the Δ*refZ* Δ*noc* and RBM_{5mu} Δ*noc* double mutants, respectively (Table 2). The increase was observed across biological and experimental replicates. We conclude that compared to wild type, Δ*refZ* Δ*noc* and RBM_{5mu} Δ*noc* double mutants show a greater proportion of cells that initiate sporulation and then fail to progress to polar division during the experimental time course.

The Δ*refZ* Δ*noc and* RBM_{5mu} Δ*noc* double mutants divide aberrantly during sporulation. At 2.5 h sporulation, the majority of wild-type and single mutant cells expressing P_{spoIIG}-*CFP* possessed an asymmetric septum or had progressed to the engulfment stage, when forespores appear rounded (Fig. 2 and Fig. S1). Asymmetric septa and engulfment were also observed in the Δ*refZ* Δ*noc* and RBM_{5mu} Δ*noc* mutants; however, unlike the single mutants, cells with abnormal morphological features were also readily observed (Fig. 2 and Fig. S1). The most frequent abnormal phenotype was a cell with two septa, one polar and one at approximately midcell of the presumed mother cell compartment (Fig. 2, yellow arrowheads & Table 2). Notably, while only 1% of wild-type cells and 1–2% of the single mutants divided aberrantly (Table 2, Class II), this percentage increased to 6% and 7% in the Δ*refZ* Δ*noc* and RBM_{5mu} Δ*noc* double mutants, respectively. A 3-fold increase in Class II divisions remained evident in the double mutants even after normalizing to the entire population of cells (dividing by the total number of Class I, II, and aseptate cells, regardless of CFP signal). We conclude that there is a synthetic interaction between the activities of

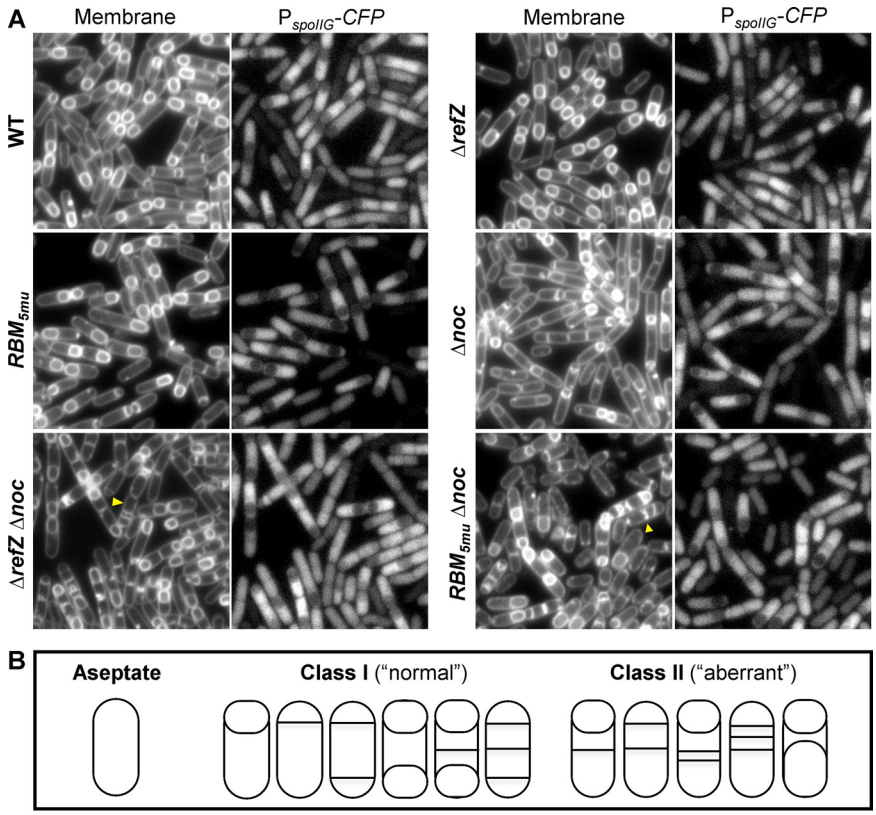

FIG 2 Expression of CFP from Spo0A-dependent promoter P_{spoIIG}. (A) Images were captured 2.5 h following sporulation by resuspension. *wt* (BAM909), Δ*refZ* (BAM1603), RBM_{5mu} (BAM910), Δ*noc* (BAM912) Δ*refZ* Δ*noc* (BAM1604), RBM_{5mu} Δ*noc* (BAM920). CFP images scaled identically to allow for direct comparison of fluorescence. All images are the same magnification. Yellow arrowheads indicate examples of aberrantly dividing cells (Class II). (B) Cell division classes during sporulation.

RefZ (likely bound at *RBM*s) and Noc that inhibits aberrant divisions during wild-type sporulation.

The Δ*noc* Δ*refZ and* RBM_{5mu} Δ*noc* double mutants activate SigF. Following polar division, sporulation progression requires activation of SigF, the first forespore-specific sigma factor. To assess if the polar compartments resembling forespores activated SigF in the mutants, we monitored expression of a SigF-dependent reporter, P_{spoIIQ}-*CFP* (61–63) using epifluorescence microscopy (Fig. 4). The percentage of cells with activated SigF across the entire population of cells with forespore-like compartments was comparable for wild type (85%), Δ*refZ* Δ*noc* (89%), and RBM_{5mu} Δ*noc* (86%) (Table 3). Consistent with our other results, only 1% of wild-type cells (4/659) exhibited aberrant (Class II) divisions, while the proportion was higher for the Δ*refZ* Δ*noc* (6%) and RBM_{5mu} Δ*noc* (7%) mutants (Fig. 4 and Table 3). In wild type, 100% (4/4) of Class II cells with apparent forespores exhibited SigF activation. By comparison, this value decreased to 39% and 56% for the Δ*refZ* Δ*noc* and RBM_{5mu} Δ*noc* mutants, respectively (Fig. 4, Table 3). We conclude that Δ*refZ* Δ*noc* and RBM_{5mu} Δ*noc* cells that divide asymmetrically are still able to activate SigF in the smaller cell compartments, but with reduced frequency compared to wild type.

RefZ's division regulation activity is required for preventing aberrant septum formation in the absence of Noc. We previously identified 10 RefZ loss-of-function variants (rLOFs) that retain the ability to bind DNA but are no longer able to perturb Z-ring assembly when artificially induced during vegetative growth (64). Cells harboring the rLOF alleles in place of wild-type *refZ* miscapture DNA in the forespore indistinguishably from the Δ*refZ* mutant, suggesting that RefZ-*RBM* complexes affect chromosome capture through direct or indirect effects on FtsZ (64). We hypothesized that RefZ's ability to

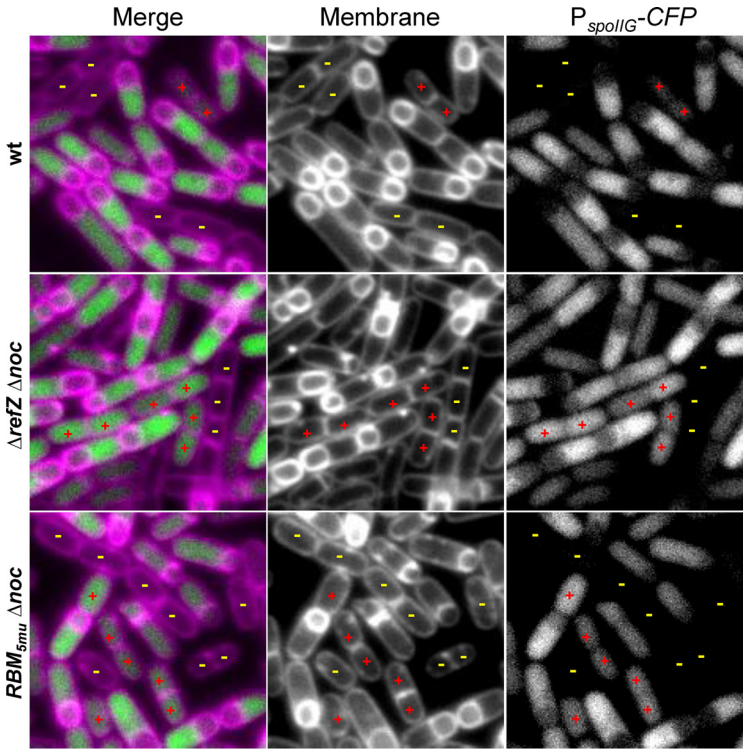

FIG 3 Expression of CFP from Spo0A-dependent promoter P_{spoIIG} in nondividing cells. Images were captured 2.5 h following sporulation by resuspension. *wt* (BAM909), Δ*refZ* Δ*noc* (BAM1604), RBM_{5mu} Δ*noc* (BAM920). Membranes were stained with TMA. CFP images scaled identically to allow for direct comparison of fluorescence. All images are the same magnification. Yellow dashes indicate examples of nondividing cells scored as CFP (−). Red plus signs indicate examples of nondividing cells scored as CFP (+).

modulate FtsZ activity would also be required to prevent aberrant divisions in the absence of *noc*. To test, we first replaced native *refZ* with each of the 10 rLOF alleles in a Δ*noc* background and evaluated sporulation using the plate-based P_{cotD}-*lacZ* assay. In the presence of wild-type *noc*, each of the rLOF encoding variants supported sporulation at levels indistinguishable from wild type (wt) or a strain encoding wild-type *refZ* linked to a chloramphenicol resistance cassette (WT), which is isogenic to the rLOF strains (Fig. 5). Conversely, none of the rLOF variants supported wild-type sporulation in a Δ*noc* background (Fig. 5), as observed with the Δ*refZ* Δ*noc* and RBM_{5mu} Δ*noc* double mutants (Fig. 1). These results suggest RefZ's ability to affect FtsZ is also required to support wild-type sporulation in the absence of Noc.

To determine whether the sporulation defect observed in the rLOF Δ*noc* double mutants also resulted in increased aberrant divisions, we monitored division in sporulating cells using fluorescence microscopy. Aberrant divisions were rarely observed in

TABLE 2 Cell division and P_{spoIIG}-*CFP* signal classes during sporulation

Genotype	Aseptate n (aseptate/total) %	Class I n (class I/total) % (class I/class I&II) %	Class II n (class II/total) % (class II/class I&II) %	CFP (+) [a]n = all cells ([a]n/total) %	CFP (+) [b]n = aseptate ([b]n/total) % ([b]n/[a]n) % ([b]n/aseptate) %
wt	355 (29)	844 (70) (99)	6 (<1) (1)	888 (74)	38 (3) (4) (11)
Δ*refZ*	345 (27)	945 (73) (99)	11 (1) (1)	998 (77)	42 (3) (4) (12)
RBM_{5mu}	461 (36)	822 (64) (99)	5 (<1) (1)	852 (66)	25 (2) (3) (5)
Δ*noc*	440 (39)	681 (60) (98)	12 (1) (2)	733 (65)	40 (4) (5) (9)
Δ*refZ* Δ*noc*	518 (44)	628 (53) (94)	40 (3) (6)	856 (72)	188 (16) (22) (36)
RBM_{5mu} Δ*noc*	628 (57)	448 (40) (92)	37 (3) (8)	821 (74)	336 (30) (41) (54)

[a]Total number of cells in the population (sum of aseptate, class I, and class II) that categorize as CFP (+). All class I & II cells categorize as CFP (+).
[b]Total number of aseptate cells that categorize as CFP (+).

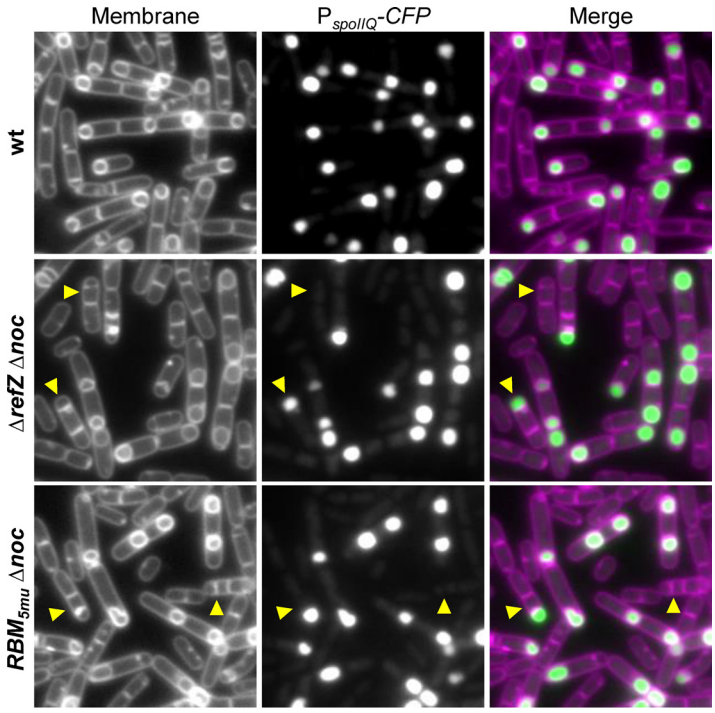

FIG 4 Expression from P_{spoIIQ}-*CFP*, a SigF-dependent reporter. Images were captured 2.5 h following sporulation by resuspension. WT (BAM1638), Δ*refZ* Δ*noc* (BAM1639), *RBM*$_{5mu}$ Δ*noc* (BAM1640). Membranes were stained with TMA. CFP channels are scaled identically to allow for direct comparison. Images are identical magnification. Yellow arrowheads indicate examples of aberrantly dividing cells (Class II).

the isogenic wild-type *refZ* strain or the rLOF mutant strains; however, when paired with Δ*noc*, each of the rLOF mutants phenocopied the Δ*refZ* Δ*noc* and *RBM*$_{5mu}$ Δ*noc* double mutants (Fig. 5). We conclude that the residues of RefZ that are required to affect division and support wild-type chromosome capture are also required to prevent abnormal divisions during sporulation in the absence of *noc*.

DISCUSSION

Both RefZ and Noc are DNA-binding proteins previously implicated in FtsZ regulation. RefZ is expressed early in sporulation and facilitates both timely polar Z-ring assembly (52) and precise capture of DNA in the forespore (51). A Δ*refZ* mutant sporulates with wild-type efficiency, so the functional significance of RefZ activity during sporulation remains unclear (52). Noc is also expressed during sporulation but to our knowledge has not previously been associated with a sporulation function. Here, we find that deleting both *noc* and *refZ* results in a synthetic sporulation defect characterized by aberrant divisions and stalled sporulation progression.

We observed several types of sporulation defects in the Δ*refZ* Δ*noc* mutant, each of which may contribute to the reduced sporulation observed in the plate-based assay. In one type, cells initiated the sporulation program, but failed to divide polarly. In a second, cells initiated sporulation and divided polarly, but failed to activate SigF, the first forespore-specific sigma factor. The largest observed category of aberrant cells divided

TABLE 3 Cell division and P_{spoIIQ}-*CFP* forespore signal (SigF activation) classes during sporulation

Genotype	Class I "normal" *n* (% class I&II)	Class II "aberrant" *n* (% class I&II)	CFP (+) *n* (% class I&II) (% class II)	CFP (−)*n* (% class I&II) (% class II)
wt	655 (99)	4 (1)	563 (85) (100)	96 (15) (0)
Δ*refZ* Δ*noc*	445 (93)	36 (7)	430 (89) (61)	51 (11) (39)
RBM$_{5mu}$ Δ*noc*	528 (94)	36 (6)	487 (86) (44)	77 (14) (56)

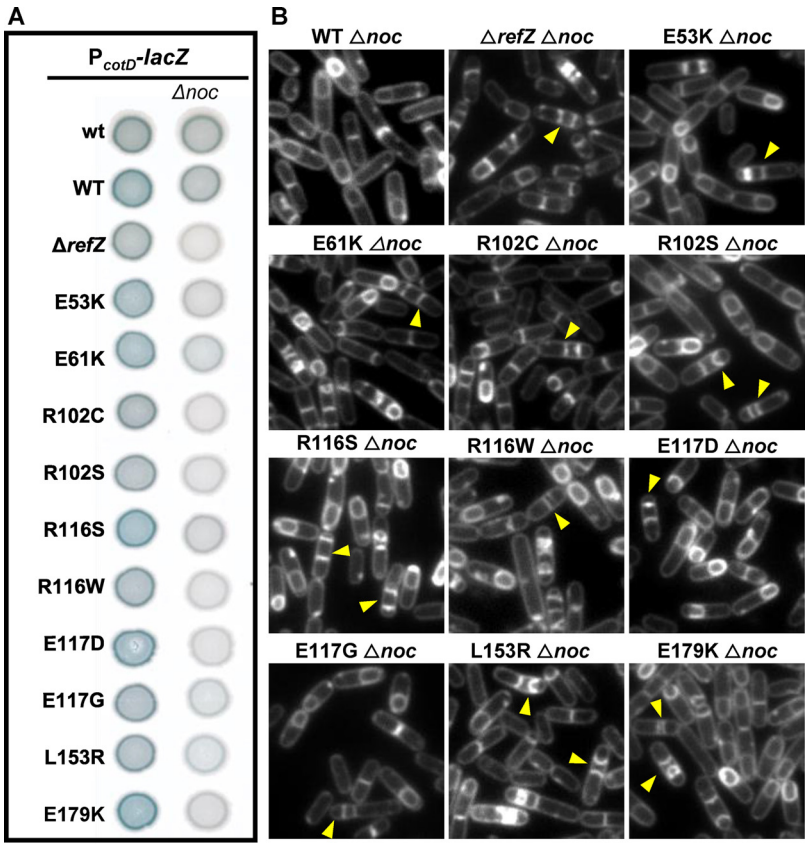

FIG 5 RefZ *LOFs* phenocopy Δ*refZ* with respect to supporting sporulation in the absence of *noc*. (A) Plate-based sporulation assay based on *lacZ* expression from a late-stage sporulation promoter, P_{cotD}. Wild-type (wt) is strain encoding wild-type *refZ*. WT is *refZ* with genetic linkage a chloramphenicol resistance cassette (isogenic to the rLOF strains). (B) Images were captured 3.5 h following sporulation by resuspension. Membranes were stained with TMA. All images are at identical magnification. Yellow arrowheads indicate examples of aberrant (Class II) divisions.

polarly and activated SigF, but also possessed an extra septum near midcell. Some of these extra septa appear to curve at later time points, reminiscent of early engulfment (several examples can be seen in Fig. 5). The "mother" cell chromosome may be pumped into the forespore-distal compartment in these cells. If so, the curvature might be explained if the center compartment attempted to engulf the abnormally large "twin" via residual SigE programming. We did not investigate the phenotype further in the present study but propose the Δ*refZ* Δ*noc* mutant may be useful for interrogating models of engulfment and spore morphogenesis (65).

Genetic interactions between Noc and other proteins implicated in cell division regulation have been observed previously (66, 67). Under conditions of rapid growth, a Δ*noc* Δ*minD* mutant is filamentous and lyses, suggesting interplay between the activities of Noc and MinD. Though we lack a mechanistic understanding of how Noc and RefZ influence Z-ring formation, the fact a sporulation defect was only observed when combining Δ*refZ* with Δ*noc* (Fig. 1), suggests there is some specificity to the interaction. Both RefZ and Noc spread along DNA and require DNA-binding for activity (32, 51, 52). Transcriptomic profiling and identification of the RefZ and Noc binding sites did not reveal obvious regulons (32, 43, 52). Of note, the NO protein SlmA is also not considered to be a transcription factor in *E. coli*; however, SlmA has been shown to activate chitobiose utilization in another enteric, *Vibrio cholerae* (68). It may be informative to revisit the effects of RefZ, Noc, and SlmA on transcription under various growth conditions using more modern methods (RNA-seq versus microarrays) and also

reexamine the regions where RefZ, Noc, and SlmA bind to look for relationships among the genes aside from position on the chromosome.

The *noc* gene evolved following a duplication of *spo0J* (*parB*) in the Firmicutes (69). In *B. subtilis*, Noc and Spo0J are 38% identical. Both proteins bind DNA and are regulated by CTP (70–73); however, unlike Spo0J (74–77), Noc does not appear to play a role in chromosome segregation; instead, a Δ*noc* mutant assembles aberrant Z-rings and/or divides over the chromosome, though only under conditions in which DNA replication and/or organization are perturbed (43, 78, 79). By comparison in *Staphylococcus aureus*, Δ*noc* mutants sometimes not only assemble extra Z-rings or divide over chromosomes, but also overinitiate DNA replication (79, 80). Several lines of evidence suggest that, at least in *S. aureus*, Noc's influence on Z-ring assembly is sensitive to nucleotide pools. First, in cells lacking *comEB* (encoding a putative CMP/dCMP deaminase), *noc* becomes essential (79). Characterized CMP/dCMP deaminases generate dCMP from dUMP, a precursor required for dTTP synthesis. Second, mutations in *dnaA* that reduce DNA replication initiation suppress Δ*noc* Δ*comEB* synthetic lethality and reduce the aberrant Z-rings associated with Δ*noc* (79). Third, Δ*noc* mutants are sensitized to DnaA overexpression compared to wild type (79). These results suggest that Noc has an activity that may buffer the cell against uncoordinated DNA replication and cell division. The reason for RefZ's synthetic interaction with Noc remains unclear, though it is notable that the aberrant divisions and failures to progress in sporulation also occur at a time in development when new rounds of DNA replication are inhibited (54, 65). Although *refZ* falls within the *spo0A* regulon, transcriptional profiling suggests that sporulation is only one context in which *refZ* is expressed (47–50, 81). Any future models for RefZ function would benefit from incorporating these additional expression contexts, as well as the conservation of the *RBM*s across the genus.

MATERIALS AND METHODS

General methods. Strains and details of strain construction can be found in the supplemental materials (Table S1 and Text S1). All *B. subtilis* strains were derived from *B. subtilis* 168. For microscopy, 25 mL cultures were grown in 250 mL baffled flasks placed in a 37°C in a shaking water bath. *B. subtilis* transformations were carried out as previously described (49), unless otherwise indicated. Sporulation was initiated by growing cells in CH medium followed by resuspension in sporulation medium (49). *B. subtilis* selections were carried out at the following antibiotic concentrations: 100 μg/mL spectinomycin, 7.5 μg/mL chloramphenicol, 10 μg/mL kanamycin, 10 μg/mL tetracycline, and 1 μg/mL erythromycin (erm) plus 25 μg/mL lincomycin for MLS. For transformation and selection in *E. coli*, antibiotics were included at the following concentrations: 100 μg/mL ampicillin and 25 μg/mL kanamycin.

PcotD-lacZ sporulation assay. For the spot plate sporulation assays, isolated colonies were used to inoculate 4 mL of DSM broth (49) and cultures were grown at 37°C in a roller drum to midlog phase. All samples were normalized to the lowest recorded culture OD600 and 5 μL from each dilution was spotted on DSM agar plates supplemented with 40 μg/mL X-gal (5-bromo-4-chloro-3-indolyl-β-d-galactopyranoside). Plates were incubated overnight at 37°C prior to imaging with a ScanJet G4050 flatbed scanner (Hewlett Packard) using VueScan software and medium format mode. Images were processed using Adobe Photoshop (versus 12.0) and ImageJ64 (82).

Heat-kill assay. Heat-kill assays to assess terminal sporulation were performed as described (83) except that DSM cultures were supplemented with 2.0 mg/mL tryptophan.

Fluorescence microscopy. Three hundred to 500 μL samples were harvested at 6,010 $\times$ *g* for 1 min in a tabletop microcentrifuge. Supernatants were aspirated and pellets were resuspended in 3–5 μL of 1$\times$ PBS containing 0.02 mM 1-(4-[trimethylamino] phenyl)-6-phenylhexa-1,3,5-triene (TMA-DPH) (Invitrogen). Cells were mounted on glass slides with polylysine-treated coverslips. Images were captured with NIS Elements Advanced Research software (version 4.10) on a Nikon Ti-E microscope fitted with a CFI Plan Apo lambda DM 100$\times$ objective, Prior Scientific Lumen 200 Illumination system, C-FL UV-2E/C DAPI filter cube with a neutral density filter and a C-FL Cyan GFP filter cube using a CoolSNAP HQ2 monochrome camera. Images were captured for 1 s. Images were analyzed in NIS-Elements or ImageJ64 (82). To score cells as either expressing or not expressing CFP, all images were scaled identically, blinded, and manually classified by experimenter as shown in Fig. 3. Cells that could not be individually or fully resolved due to crowding or location on the periphery of an image were not included in the quantitation.

SUPPLEMENTAL MATERIAL

Supplemental material is available online only.

SUPPLEMENTAL FILE 1, PDF file, 5.3 MB.

ACKNOWLEDGMENTS

We thank members of the Herman Lab for critical reading of the manuscript. This work was supported by a grant from the National Science Foundation to J.K.H. (MCB-1514629).

REFERENCES

1. Gueiros-Filho FJ, Losick R. 2002. A widely conserved bacterial cell division protein that promotes assembly of the tubulin-like protein FtsZ. Genes Dev 16:2544–2556. https://doi.org/10.1101/gad.1014102.
2. Monahan LG, Robinson A, Harry EJ. 2009. Lateral FtsZ association and the assembly of the cytokinetic Z ring in bacteria. Mol Microbiol 74:1004–1017. https://doi.org/10.1111/j.1365-2958.2009.06914.x.
3. Gündoğdu ME, Kawai Y, Pavlendova N, Ogasawara N, Errington J, Scheffers D-J, Hamoen LW. 2011. Large ring polymers align FtsZ polymers for normal septum formation. EMBO J 30:617–626. https://doi.org/10.1038/emboj.2010.345.
4. Hamoen LW, Meile JC, de Jong W, Noirot P, Errington J. 2006. SepF, a novel FtsZ-interacting protein required for a late step in cell division. Mol Microbiol 59:989–999. https://doi.org/10.1111/j.1365-2958.2005.04987.x.
5. Ishikawa S, Kawai Y, Hiramatsu K, Kuwano M, Ogasawara N. 2006. A new FtsZ-interacting protein, YlmF, complements the activity of FtsA during progression of cell division in *Bacillus subtilis*. Mol Microbiol 60:1364–1380. https://doi.org/10.1111/j.1365-2958.2006.05184.x.
6. Haeusser DP, Schwartz RL, Smith AM, Oates ME, Levin PA. 2004. EzrA prevents aberrant cell division by modulating assembly of the cytoskeletal protein FtsZ. Mol Microbiol 52:801–814. https://doi.org/10.1111/j.1365-2958.2004.04016.x.
7. Levin PA, Kurtser IG, Grossman AD. 1999. Identification and characterization of a negative regulator of FtsZ ring formation in *Bacillus subtilis*. Proc Natl Acad Sci U S A 96:9642–9647. https://doi.org/10.1073/pnas.96.17.9642.
8. Singh JK, Makde RD, Kumar V, Panda D. 2007. A membrane protein, EzrA, regulates assembly dynamics of FtsZ by interacting with the C-terminal tail of FtsZ. Biochemistry 46:11013–11022. https://doi.org/10.1021/bi700710j.
9. Gamba P, Veening JW, Saunders NJ, Hamoen LW, Daniel RA. 2009. Two-step assembly dynamics of the *Bacillus subtilis* divisome. J Bacteriol 191:4186–4194. https://doi.org/10.1128/JB.01758-08.
10. Beall B, Lutkenhaus J. 1991. FtsZ in *Bacillus subtilis* is required for vegetative septation and for asymmetric septation during sporulation. Genes Dev 5:447–455. https://doi.org/10.1101/gad.5.3.447.
11. Mukherjee A, Lutkenhaus J. 1998. Dynamic assembly of FtsZ regulated by GTP hydrolysis. EMBO J 17:462–469. https://doi.org/10.1093/emboj/17.2.462.
12. Pichoff S, Lutkenhaus J. 2005. Tethering the Z ring to the membrane through a conserved membrane targeting sequence in FtsA. Mol Microbiol 55:1722–1734. https://doi.org/10.1111/j.1365-2958.2005.04522.x.
13. Pichoff S, Lutkenhaus J. 2007. Identification of a region of FtsA required for interaction with FtsZ. Mol Microbiol 64:1129–1138. https://doi.org/10.1111/j.1365-2958.2007.05735.x.
14. Bisson-Filho AW, Hsu YP, Squyres GR, Kuru E, Wu F, Jukes C, Sun Y, Dekker C, Holden S, VanNieuwenhze MS, Brun YV, Garner EC. 2017. Treadmilling by FtsZ filaments drives peptidoglycan synthesis and bacterial cell division. Science 355:739–743. https://doi.org/10.1126/science.aak9973.
15. Lan G, Daniels BR, Dobrowsky TM, Wirtz D, Sun SX. 2009. Condensation of FtsZ filaments can drive bacterial cell division. Proc Natl Acad Sci U S A 106:121–126. https://doi.org/10.1073/pnas.0807963106.
16. Yang X, Lyu Z, Miguel A, McQuillen R, Huang KC, Xiao J. 2017. GTPase activity-coupled treadmilling of the bacterial tubulin FtsZ organizes septal cell wall synthesis. Science 355:744–747. https://doi.org/10.1126/science.aak9995.
17. Dominguez-Escobar J, Chastanet A, Crevenna AH, Fromion V, Wedlich-Soldner R, Carballido-Lopez R. 2011. Processive movement of MreB-associated cell wall biosynthetic complexes in bacteria. Science 333:225–228. https://doi.org/10.1126/science.1203466.
18. Garner EC, Bernard R, Wang W, Zhuang X, Rudner DZ, Mitchison T. 2011. Coupled, circumferential motions of the cell wall synthesis machinery and MreB filaments in *B. subtilis*. Science 333:222–225. https://doi.org/10.1126/science.1203285.
19. Haeusser DP, Margolin W. 2016. Splitsville: structural and functional insights into the dynamic bacterial Z ring. Nat Rev Microbiol 14:305–319. https://doi.org/10.1038/nrmicro.2016.26.
20. Stricker J, Maddox P, Salmon ED, Erickson HP. 2002. Rapid assembly dynamics of the *Escherichia coli* FtsZ-ring demonstrated by fluorescence recovery after photobleaching. Proc Natl Acad Sci U S A 99:3171–3175. https://doi.org/10.1073/pnas.052595099.
21. Rodrigues CD, Harry EJ. 2012. The Min system and nucleoid occlusion are not required for identifying the division site in *Bacillus subtilis* but ensure its efficient utilization. PLoS Genet 8:e1002561. https://doi.org/10.1371/journal.pgen.1002561.
22. Bramkamp M, van Baarle S. 2009. Division site selection in rod-shaped bacteria. Curr Opin Microbiol 12:683–688. https://doi.org/10.1016/j.mib.2009.10.002.
23. van Baarle S, Bramkamp M. 2010. The MinCDJ system in *Bacillus subtilis* prevents minicell formation by promoting divisome disassembly. PLoS One 5:e9850. https://doi.org/10.1371/journal.pone.0009850.
24. Bramkamp M, Emmins R, Weston L, Donovan C, Daniel RA, Errington J. 2008. A novel component of the division-site selection system of *Bacillus subtilis* and a new mode of action for the division inhibitor MinCD. Mol Microbiol 70:1556–1569. https://doi.org/10.1111/j.1365-2958.2008.06501.x.
25. Eswaramoorthy P, Erb ML, Gregory JA, Silverman J, Pogliano K, Pogliano J, Ramamurthi KS. 2011. Cellular architecture mediates DivIVA ultrastructure and regulates min activity in *Bacillus subtilis*. mBio 2. https://doi.org/10.1128/mBio.00257-11.
26. Patrick JE, Kearns DB. 2008. MinJ (YvjD) is a topological determinant of cell division in *Bacillus subtilis*. Mol Microbiol 70:1166–1179. https://doi.org/10.1111/j.1365-2958.2008.06469.x.
27. Ramamurthi KS, Losick R. 2009. Negative membrane curvature as a cue for subcellular localization of a bacterial protein. Proc Natl Acad Sci U S A 106:13541–13545. https://doi.org/10.1073/pnas.0906851106.
28. Gregory JA, Becker EC, Pogliano K. 2008. *Bacillus subtilis* MinC destabilizes FtsZ-rings at new cell poles and contributes to the timing of cell division. Genes Dev 22:3475–3488. https://doi.org/10.1101/gad.1732408.
29. Cho H, McManus HR, Dove SL, Bernhardt TG. 2011. Nucleoid occlusion factor SlmA is a DNA-activated FtsZ polymerization antagonist. Proc Natl Acad Sci U S A 108:3773–3778. https://doi.org/10.1073/pnas.1018674108.
30. Bernhardt TG, de Boer PA. 2005. SlmA, a nucleoid-associated, FtsZ binding protein required for blocking septal ring assembly over chromosomes in *E. coli*. Mol Cell 18:555–564. https://doi.org/10.1016/j.molcel.2005.04.012.
31. Tonthat NK, Arold ST, Pickering BF, Van Dyke MW, Liang S, Lu Y, Beuria TK, Margolin W, Schumacher MA. 2011. Molecular mechanism by which the nucleoid occlusion factor, SlmA, keeps cytokinesis in check. EMBO J 30:154–164. https://doi.org/10.1038/emboj.2010.288.
32. Wu LJ, Ishikawa S, Kawai Y, Oshima T, Ogasawara N, Errington J. 2009. Noc protein binds to specific DNA sequences to coordinate cell division with chromosome segregation. EMBO J 28:1940–1952. https://doi.org/10.1038/emboj.2009.144.
33. Adams DW, Wu LJ, Errington J. 2015. Nucleoid occlusion protein Noc recruits DNA to the bacterial cell membrane. EMBO J 34:491–501. https://doi.org/10.15252/embj.201490177.
34. Yu Y, Zhou J, Gueiros-Filho FJ, Kearns DB, Jacobson SC. 2021. Noc Corrals Migration of FtsZ Protofilaments during Cytokinesis in *Bacillus subtilis*. mBio 12. https://doi.org/10.1128/mBio.02964-20.
35. Hilbert DW, Piggot PJ. 2004. Compartmentalization of gene expression during *Bacillus subtilis* spore formation. Microbiol Mol Biol Rev 68:234–262. https://doi.org/10.1128/MMBR.68.2.234-262.2004.
36. Khvorova A, Zhang L, Higgins ML, Piggot PJ. 1998. The *spoIIE* locus is involved in the Spo0A-dependent switch in the location of FtsZ rings in *Bacillus subtilis*. J Bacteriol 180:1256–1260. https://doi.org/10.1128/JB.180.5.1256-1260.1998.
37. Levin PA, Losick R. 1996. Transcription factor Spo0A switches the localization of the cell division protein FtsZ from a medial to a bipolar pattern in

Bacillus subtilis. Genes Dev 10:478–488. https://doi.org/10.1101/gad.10.4.478.
38. Piggot PJ, Coote JG. 1976. Genetic aspects of bacterial endospore formation. Bacteriol Rev 40:908–962. https://doi.org/10.1128/br.40.4.908-962.1976.
39. Fiche JB, Cattoni DI, Diekmann N, Langerak JM, Clerte C, Royer CA, Margeat E, Doan T, Nollmann M. 2013. Recruitment, assembly, and molecular architecture of the SpoIIIE DNA pump revealed by superresolution microscopy. PLoS Biol 11:e1001557. https://doi.org/10.1371/journal.pbio.1001557.
40. Wu LJ, Errington J. 1994. *Bacillus subtilis* SpoIIIE protein required for DNA segregation during asymmetric cell division. Science 264:572–575. https://doi.org/10.1126/science.8160014.
41. Wu LJ, Errington J. 1997. Septal localization of the SpoIIIE chromosome partitioning protein in *Bacillus subtilis*. EMBO J 16:2161–2169. https://doi.org/10.1093/emboj/16.8.2161.
42. Wu LJ, Errington J. 1998. Use of asymmetric cell division and *spoIIIE* mutants to probe chromosome orientation and organization in *Bacillus subtilis*. Mol Microbiol 27:777–786. https://doi.org/10.1046/j.1365-2958.1998.00724.x.
43. Wu LJ, Errington J. 2004. Coordination of cell division and chromosome segregation by a nucleoid occlusion protein in *Bacillus subtilis*. Cell 117:915–925. https://doi.org/10.1016/j.cell.2004.06.002.
44. Gonzy-Treboul G, Karmazyn-Campelli C, Stragier P. 1992. Developmental regulation of transcription of the *Bacillus subtilis ftsAZ* operon. J Mol Biol 224:967–979. https://doi.org/10.1016/0022-2836(92)90463-t.
45. Carniol K, Ben-Yehuda S, King N, Losick R. 2005. Genetic dissection of the sporulation protein SpoIIE and its role in asymmetric division in *Bacillus subtilis*. J Bacteriol 187:3511–3520. https://doi.org/10.1128/JB.187.10.3511-3520.2005.
46. Ben-Yehuda S, Losick R. 2002. Asymmetric cell division in *B. subtilis* involves a spiral-like intermediate of the cytokinetic protein FtsZ. Cell 109:257–266. https://doi.org/10.1016/S0092-8674(02)00698-0.
47. Molle V, Fujita M, Jensen ST, Eichenberger P, Gonzalez-Pastor JE, Liu JS, Losick R. 2003. The Spo0A regulon of *Bacillus subtilis*. Mol Microbiol 50:1683–1701. https://doi.org/10.1046/j.1365-2958.2003.03818.x.
48. Blencke HM, Homuth G, Ludwig H, Mader U, Hecker M, Stulke J. 2003. Transcriptional profiling of gene expression in response to glucose in *Bacillus subtilis*: regulation of the central metabolic pathways. Metab Eng 5:133–149. https://doi.org/10.1016/s1096-7176(03)00009-0.
49. Harwood CR, Cutting SM. 1990. Molecular biological methods for Bacillus. Wiley, New York, NY.
50. Britton RA, Lin DC, Grossman AD. 1998. Characterization of a prokaryotic SMC protein involved in chromosome partitioning. Genes Dev 12:1254–1259. https://doi.org/10.1101/gad.12.9.1254.
51. Miller AK, Brown EE, Mercado BT, Herman JK. 2016. A DNA-binding protein defines the precise region of chromosome capture during *Bacillus* sporulation. Mol Microbiol 99:111–122. https://doi.org/10.1111/mmi.13217.
52. Wagner-Herman JK, Bernard R, Dunne R, Bisson-Filho AW, Kumar K, Nguyen T, Mulcahy L, Koullias J, Gueiros-Filho FJ, Rudner DZ. 2012. RefZ facilitates the switch from medial to polar division during spore formation in *Bacillus subtilis*. J Bacteriol 194:4608–4618. https://doi.org/10.1128/JB.00378-12.
53. Barak I, Muchova K. 2018. The positioning of the asymmetric septum during sporulation in *Bacillus subtilis*. PLoS One 13:e0201979. https://doi.org/10.1371/journal.pone.0201979.
54. Wagner JK, Marquis KA, Rudner DZ. 2009. SirA enforces diploidy by inhibiting the replication initiator DnaA during spore formation in *Bacillus subtilis*. Mol Microbiol 73:963–974. https://doi.org/10.1111/j.1365-2958.2009.06825.x.
55. Barak I, Prepiak P, Schmeisser F. 1998. MinCD proteins control the septation process during sporulation of *Bacillus subtilis*. J Bacteriol 180:5327–5333. https://doi.org/10.1128/JB.180.20.5327-5333.1998.
56. Kloosterman TG, Lenarcic R, Willis CR, Roberts DM, Hamoen LW, Errington J, Wu LJ. 2016. Complex polar machinery required for proper chromosome segregation in vegetative and sporulating cells of *Bacillus subtilis*. Mol Microbiol 101:333–350. https://doi.org/10.1111/mmi.13393.
57. Duan Y, Huey JD, Herman JK. 2016. The DnaA inhibitor SirA acts in the same pathway as Soj (ParA) to facilitate *oriC* segregation during *Bacillus subtilis* sporulation. Mol Microbiol 102:530–544. https://doi.org/10.1111/mmi.13477.
58. Wu LJ, Errington J. 2003. RacA and the Soj-Spo0J system combine to effect polar chromosome segregation in sporulating *Bacillus subtilis*. Mol Microbiol 49:1463–1475. https://doi.org/10.1046/j.1365-2958.2003.03643.x.
59. Dworkin J, Losick R. 2005. Developmental commitment in a bacterium. Cell 121:401–409. https://doi.org/10.1016/j.cell.2005.02.032.
60. Fujita M, Gonzalez-Pastor JE, Losick R. 2005. High- and low-threshold genes in the Spo0A regulon of *Bacillus subtilis*. J Bacteriol 187:1357–1368. https://doi.org/10.1128/JB.187.4.1357-1368.2005.
61. Wang ST, Setlow B, Conlon EM, Lyon JL, Imamura D, Sato T, Setlow P, Losick R, Eichenberger P. 2006. The forespore line of gene expression in *Bacillus subtilis*. J Mol Biol 358:16–37. https://doi.org/10.1016/j.jmb.2006.01.059.
62. Londono-Vallejo JA, Frehel C, Stragier P. 1997. SpoIIQ, a forespore-expressed gene required for engulfment in *Bacillus subtilis*. Mol Microbiol 24:29–39. https://doi.org/10.1046/j.1365-2958.1997.3181680.x.
63. Steil L, Serrano M, Henriques AO, Volker U. 2005. Genome-wide analysis of temporally regulated and compartment-specific gene expression in sporulating cells of *Bacillus subtilis*. Microbiology (Reading) 151:399–420. https://doi.org/10.1099/mic.0.27493-0.
64. Brown EE, Miller AK, Krieger IV, Otto RM, Sacchettini JC, Herman JK. 2019. A DNA-Binding protein tunes septum placement during *Bacillus subtilis* Sporulation. J Bacteriol 201. https://doi.org/10.1128/JB.00287-19.
65. Khanna K, Lopez-Garrido J, Pogliano K. 2020. Shaping an endospore: architectural transformations during *Bacillus subtilis* sporulation. Annu Rev Microbiol 74:361–386. https://doi.org/10.1146/annurev-micro-022520-074650.
66. Surdova K, Gamba P, Claessen D, Siersma T, Jonker MJ, Errington J, Hamoen LW. 2013. The conserved DNA-binding protein WhiA is involved in cell division in *Bacillus subtilis*. J Bacteriol 195:5450–5460. https://doi.org/10.1128/JB.00507-13.
67. Yu Y, Dempwolff F, Oshiro RT, Gueiros-Filho FJ, Jacobson SC, Kearns DB. 2021. The division defect of a *Bacillus subtilis minD noc* double mutant can be suppressed by Spx-dependent and Spx-independent mechanisms. J Bacteriol 203:e0024921. https://doi.org/10.1128/JB.00249-21.
68. Klancher CA, Hayes CA, Dalia AB. 2017. The nucleoid occlusion protein SlmA is a direct transcriptional activator of chitobiose utilization in *Vibrio cholerae*. PLoS Genet 13:e1006877. https://doi.org/10.1371/journal.pgen.1006877.
69. Ogasawara N, Yoshikawa H. 1992. Genes and their organization in the replication origin region of the bacterial chromosome. Mol Microbiol 6:629–634. https://doi.org/10.1111/j.1365-2958.1992.tb01510.x.
70. Antar H, Soh YM, Zamuner S, Bock FP, Anchimiuk A, Rios PL, Gruber S. 2021. Relief of ParB autoinhibition by *parS* DNA catalysis and recycling of ParB by CTP hydrolysis promote bacterial centromere assembly. Sci Adv 7:eabj2854. https://doi.org/10.1126/sciadv.abj2854.
71. Taylor JA, Seol Y, Budhathoki J, Neuman KC, Mizuuchi K. 2021. CTP and *parS* coordinate ParB partition complex dynamics and ParA-ATPase activation for ParABS-mediated DNA partitioning. Elife 10. https://doi.org/10.7554/eLife.65651.
72. Jalal ASB, Tran NT, Wu LJ, Ramakrishnan K, Rejzek M, Gobbato G, Stevenson CEM, Lawson DM, Errington J, Le TBK. 2021. CTP regulates membrane-binding activity of the nucleoid occlusion protein Noc. Mol Cell 81:3623–3636. https://doi.org/10.1016/j.molcel.2021.06.025.
73. Osorio-Valeriano M, Altegoer F, Steinchen W, Urban S, Liu Y, Bange G, Thanbichler M. 2019. ParB-type DNA segregation proteins are CTP-dependent molecular switches. Cell 179:1512–1524. https://doi.org/10.1016/j.cell.2019.11.015.
74. Ireton K, Gunther NWt, Grossman AD. 1994. *spo0J* is required for normal chromosome segregation as well as the initiation of sporulation in *Bacillus subtilis*. J Bacteriol 176:5320–5329. https://doi.org/10.1128/jb.176.17.5320-5329.1994.
75. Lee PS, Grossman AD. 2006. The chromosome partitioning proteins Soj (ParA) and Spo0J (ParB) contribute to accurate chromosome partitioning, separation of replicated sister origins, and regulation of replication initiation in *Bacillus subtilis*. Mol Microbiol 60:853–869. https://doi.org/10.1111/j.1365-2958.2006.05140.x.
76. Sullivan NL, Marquis KA, Rudner DZ. 2009. Recruitment of SMC by ParB-parS organizes the origin region and promotes efficient chromosome segregation. Cell 137:697–707. https://doi.org/10.1016/j.cell.2009.04.044.
77. Gruber S, Errington J. 2009. Recruitment of condensin to replication origin regions by ParB/SpoOJ promotes chromosome segregation in *B. subtilis*. Cell 137:685–696. https://doi.org/10.1016/j.cell.2009.02.035.
78. Biller SJ, Burkholder WF. 2009. The *Bacillus subtilis* SftA (YtpS) and SpoIIIE DNA translocases play distinct roles in growing cells to ensure faithful

chromosome partitioning. Mol Microbiol 74:790–809. https://doi.org/10.1111/j.1365-2958.2009.06893.x.
79. Pang T, Wang X, Lim HC, Bernhardt TG, Rudner DZ. 2017. The nucleoid occlusion factor Noc controls DNA replication initiation in *Staphylococcus aureus*. PLoS Genet 13:e1006908. https://doi.org/10.1371/journal.pgen.1006908.
80. Veiga H, Jorge AM, Pinho MG. 2011. Absence of nucleoid occlusion effector Noc impairs formation of orthogonal FtsZ rings during *Staphylococcus aureus* cell division. Mol Microbiol 80:1366–1380. https://doi.org/10.1111/j.1365-2958.2011.07651.x.
81. Nicolas P, Mäder U, Dervyn E, Rochat T, Leduc A, Pigeonneau N, Bidnenko E, Marchadier E, Hoebeke M, Aymerich S, Becher D, Bisicchia P, Botella E, Delumeau O, Doherty G, Denham EL, Fogg MJ, Fromion V, Goelzer A, Hansen A, Härtig E, Harwood CR, Homuth G, Jarmer H, Jules M, Klipp E, Le Chat L, Lecointe F, Lewis P, Liebermeister W, March A, Mars RAT, Nannapaneni P, Noone D, Pohl S, Rinn B, Rügheimer F, Sappa PK, Samson F, Schaffer M, Schwikowski B, Steil L, Stülke J, Wiegert T, Devine KM, Wilkinson AJ, van Dijl JM, Hecker M, Völker U, Bessières P, et al. 2012. Condition-dependent transcriptome reveals high-level regulatory architecture in *Bacillus subtilis*. Science 335:1103–1106. https://doi.org/10.1126/science.1206848.
82. Rasband WS. 1997–2018. ImageJ, on U. S. National Institutes of Health, Bethesda, Maryland. https://imagej.nih.gov/ij/.
83. Duan Y, Sperber AM, Herman JK. 2016. YodL and YisK possess shape-modifying activities that are suppressed by mutations in *Bacillus subtilis mreB* and *mbl*. J Bacteriol 198:2074–2088. https://doi.org/10.1128/JB.00183-16.

Supplementary materials

RefZ and Noc act synthetically to prevent aberrant divisions during *Bacillus subtilis* sporulation

Allyssa K. Miller and Jennifer K. Herman*

Department of Biochemistry and Biophysics, Texas A&M University, College Station, TX

Corresponding author*

Short title: Septation during *B. subtilis* sporulation

Figure S1. Expression of CFP from Spo0A-dependent promoter P_{spoIIG} 2.5 hr following sporulation by resuspension.
Table S1. Strains
Text S1. Strain construction

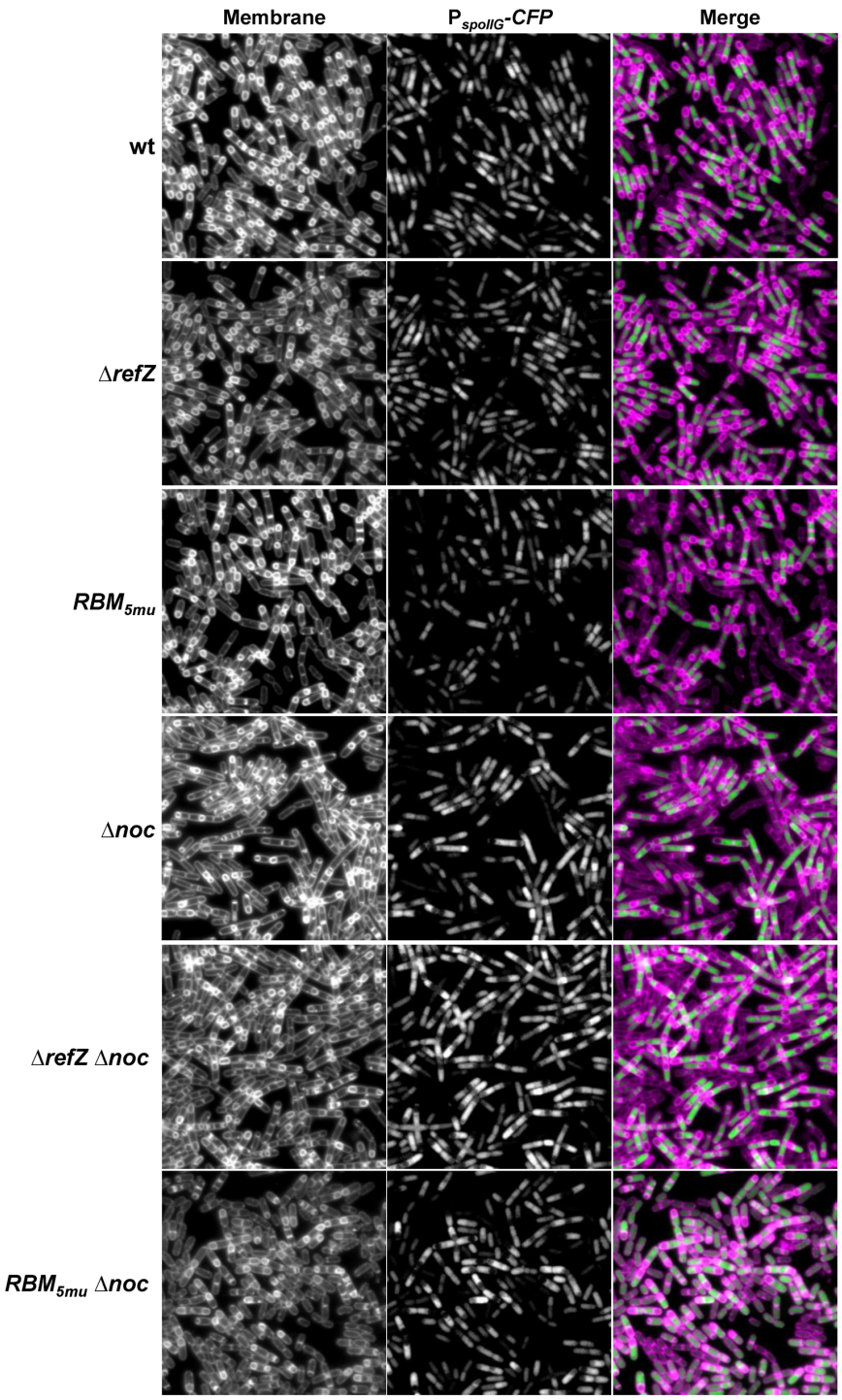

Figure S1. Expression of CFP from Spo0A-dependent promoter P_{spoIIG} 2.5 hr following sporulation by resuspension. CFP images are scaled identically to allow for direct comparison of fluorescence. WT (BAM909), Δ*refZ* (BAM1603), RBM_{5mu} (BAM910), Δ*noc* (BAM912) Δ*refZ* Δ*noc* (BAM1604), RBM_{5mu} Δ*noc* (BAM920).

Table S1. Strains

***Bacillus subtilis* 168**	Corresponds to strain stored at the *Bacillus* Genetic Stock Center under accession number 1A1. Unlike the reference genome, this strain encodes full-length SwrA.	
BAM043	*minD::kan*	
BAM067	*amyE::P_{spoIIQ}-cfp (cat)*	
BAM118	*ezrA::kan*	
BAM125	*RBM_{5mu}, ezrA::kan*	
BAM226	*RBM_{5mu}, sepF::erm*	
BAM325	*noc::erm*	
BAM469	*Δ(soj-spo0J)::cat, pelB::spo0J (kan)*	
BAM908	*RBM_{5mu}, noc::erm*	
BAM909	*amyE::P_{spoIIG}-cfp (spec)*	Fig 2, 3, S1
BAM910	*RBM_{5mu}, amyE::P_{spoIIG}-cfp (spec)*	Fig 2, 3, S1
BAM912	*amyE::P_{spoIIG}-cfp (spec), noc::erm*	Fig 2, 3, S1
BAM920	*RBM_{5mu}, amyE::P_{spoIIG}-cfp (spec), noc::erm*	Fig 2, 3, S1
BAM1265	*refZ::refZ (WT)(cat)*	
BAM1266	*refZ::refZ (E53K)(cat)*	
BAM1267	*refZ::refZ (E61K)(cat)*	
BAM1268	*refZ::refZ (R102C)(cat)*	
BAM1269	*refZ::refZ (R102S)(cat)*	
BAM1270	*refZ::refZ (R116S)(cat)*	
BAM1271	*refZ::refZ (R116W)(cat)*	
BAM1272	*refZ::refZ (E117D)(cat)*	
BAM1273	*refZ::refZ (E117G)(cat)*	
BAM1274	*refZ::refZ (L153R)(cat)*	
BAM1275	*refZ::refZ (E179K)(cat)*	
BAM1280	*refZ::refZ (WT)(cat), noc::erm*	Fig 5B
BAM1281	*refZ::refZ (E53K)(cat), noc::erm*	Fig 5B
BAM1282	*refZ::refZ (E61K)(cat), noc::erm*	Fig 5B
BAM1283	*refZ::refZ (R102C)(cat), noc::erm*	Fig 5B
BAM1284	*refZ::refZ (R102S)(cat), noc::erm*	Fig 5B
BAM1285	*refZ::refZ (R116S)(cat), noc::erm*	Fig 5B
BAM1286	*refZ::refZ (R116W)(cat), noc::erm*	Fig 5B
BAM1287	*refZ::refZ (E117D)(cat), noc::erm*	Fig 5B
BAM1288	*refZ::refZ (E117G)(cat), noc::erm*	Fig 5B
BAM1289	*refZ::refZ (L153R)(cat), noc::erm*	Fig 5B
BAM1290	*refZ::refZ (E179K)(cat), noc::erm*	Fig 5B
BAM1295	*refZ::cat, noc::erm*	
BAM1296	*refZ::erm*	

BAM1305	*refZ::refZ (WT)(cat), noc::erm, amyE::P_{cotD}-lacZ (spec)*	Fig 5A
BAM1306	*refZ::refZ (E53K)(cat), noc::erm, amyE::P_{cotD}-lacZ (spec)*	Fig 5A
BAM1307	*refZ::refZ (E61K)(cat), noc::erm, amyE::P_{cotD}-lacZ (spec)*	Fig 5A
BAM1308	*refZ::refZ (R102C)(cat), noc::erm, amyE::P_{cotD}-lacZ (spec)*	Fig 5A
BAM1309	*refZ::refZ (R102S)(cat), noc::erm, amyE::P_{cotD}-lacZ (spec)*	Fig 5A
BAM1310	*refZ::refZ (R116S)(cat), noc::erm, amyE::P_{cotD}-lacZ (spec)*	Fig 5A
BAM1311	*refZ::refZ (R116W)(cat), noc::erm, amyE::P_{cotD}-lacZ (spec)*	Fig 5A
BAM1312	*refZ::refZ (E117D)(cat), noc::erm, amyE::P_{cotD}-lacZ (spec)*	Fig 5A
BAM1313	*refZ::refZ (E117G)(cat), noc::erm, amyE::P_{cotD}-lacZ (spec)*	Fig 5A
BAM1314	*refZ::refZ (L153R)(cat), noc::erm, amyE::P_{cotD}-lacZ (spec)*	Fig 5A
BAM1315	*refZ::refZ (E179K)(cat), noc::erm, amyE::P_{cotD}-lacZ (spec)*	Fig 5A
BAM1320	*refZ::cat, noc::erm, amyE::P_{cotD}-lacZ (spec)*	Fig 5A
BAM1321	*noc::erm, amyE::P_{cotD}-lacZ (spec)*	Fig 1, 5A
BAM1322	*refZ::cat, amyE::P_{cotD}-lacZ (spec)*	Fig 5A
BAM1323	*amyE::P_{cotD}-lacZ (spec)*	Fig 1, 5A
BAM1324	*refZ::refZ (WT)(cat), amyE::P_{cotD}-lacZ (spec)*	Fig 5A
BAM1325	*refZ::refZ (E53K)(cat), amyE::P_{cotD}-lacZ (spec)*	Fig 5A
BAM1326	*refZ::refZ (E61K)(cat), amyE::P_{cotD}-lacZ (spec)*	Fig 5A
BAM1327	*refZ::refZ (R102C)(cat), amyE::P_{cotD}-lacZ (spec)*	Fig 5A
BAM1328	*refZ::refZ (R102S)(cat), amyE::P_{cotD}-lacZ (spec)*	Fig 5A
BAM1329	*refZ::refZ (R116S)(cat), amyE::P_{cotD}-lacZ (spec)*	Fig 5A
BAM1330	*refZ::refZ (R116W)(cat), amyE::P_{cotD}-lacZ (spec)*	Fig 5A
BAM1331	*refZ::refZ (E117D)(cat), amyE::P_{cotD}-lacZ (spec)*	Fig 5A
BAM1332	*refZ::refZ (E117G)(cat), amyE::P_{cotD}-lacZ (spec)*	Fig 5A
BAM1333	*refZ::refZ (L153R)(cat), amyE::P_{cotD}-lacZ (spec)*	Fig 5A
BAM1334	*refZ::refZ (E179K)(cat), amyE::P_{cotD}-lacZ (spec)*	Fig 5A
BAM1339	*ΔrefZ*	
BAM1359	*ΔrefZ, noc::erm*	
BAM1409	*ΔrefZ, minD::kan*	
BAM1529	*ΔrefZ, ezrA::kan*	
BAM1546	*ΔrefZ, noc::erm, amyE::P_{cotD}-lacZ (spec)*	Fig 1
BAM1547	*RBM_{5mu}, sepF::erm, amyE::P_{cotD}-lacZ (spec)*	Fig 1
BAM1548	*sepF::erm, amyE::P_{cotD}-lacZ (spec)*	Fig 1
BAM1549	*Δ(soj-spo0J)::cat, pelB::spo0J (kan), amyE::P_{cotD}-lacZ (spec)*	Fig 1
BAM1550	*ΔrefZ, amyE::P_{cotD}-lacZ (spec)*	Fig 1
BAM1557	*ΔrefZ, sepF::erm*	
BAM1559	*ΔrefZ, ezrA::kan, amyE::P_{cotD}-lacZ (spec)*	Fig 1
BAM1562	*RBM_{5mu}, noc::erm, amyE::P_{cotD}-lacZ (spec)*	Fig 1
BAM1563	*ezrA::kan, amyE::P_{cotD}-lacZ (spec)*	Fig 1
BAM1564	*RBM_{5mu}, ezrA::kan, amyE::P_{cotD}-lacZ (spec)*	Fig 1

BAM1566	*ΔrefZ, Δ(soj-spo0J)::cat, pelB::spo0J (kan)*	
BAM1567	*RBM_{5mu}, Δ(soj-spo0J)::cat, pelB::spo0J (kan)*	
BAM1568	*ΔrefZ, Δ(soj-spo0J)::cat, pelB::spo0J (kan), amyE::PcotD-lacZ (spec)*	Fig 1
BAM1569	*RBM_{5mu}, Δ(soj-spo0J)::cat, pelB::spo0J (kan), amyE::P_{cotD}-lacZ (spec)*	Fig 1
BAM1573	*RBM_{5mu}, amyE::P_{cotD}-lacZ (spec)*	Fig 1
BAM1575	*amyE::P_{cotD}-lacZ (spec), minD::kan*	Fig 1
BAM1576	*RBM_{5mu}, amyE::P_{cotD}-lacZ (spec), minD::kan*	Fig 1
BAM1577	*ΔrefZ, sepF::erm, amyE::P_{cotD}-lacZ (spec)*	Fig 1
BAM1578	*ΔrefZ, minD::kan, amyE::P_{cotD}-lacZ (spec)*	Fig 1
BAM1600	*refZ::tet, amyE::P_{spoIIQ}-cfp (cat)*	
BAM1601	*RBM_{5mu}, amyE::$_{PspoIIQ}$-cfp (cat)*	
BAM1603	*amyE::P_{spoIIG}-cfp (spec), refZ::tet*	Fig 2, 3
BAM1604	*amyE::P_{spoIIG}-cfp (spec), noc::erm, refZ::tet*	Fig 2, 3
BAM1610	*refZ::tet, amyE::P_{spoIIQ}-cfp (cat), noc::erm*	
BAM1611	*RBM_{5mu}, amyE::$_{PspoIIQ}$-cfp (cat), noc::erm*	
BAM1638	*amyE::P_{spoIIQ}-cfp (cat), rpoC-gfp (spec)*	Fig 4
BAM1639	*refZ::tet, amyE::P_{spoIIQ}-cfp (cat), noc::erm, rpoC-gfp (spec)*	Fig 4
BAM1640	*RBM_{5mu}, amyE::$_{PspoIIQ}$-cfp (cat), noc::erm, rpoC-gfp (spec)*	Fig 4
BJH205	*RBM_{5mu}*	(1)
BJH358	*sepF::erm* (BKE15390)	(2)

Text S1. Strain construction

BAM043 [*minD::kan*] was created by transforming *Bs168* with genomic DNA from BDR2353 [*PY79 minD::kan*] selecting for growth on LB plates containing 10 µg/ml kanamycin.

BAM067 [*amyE::PspoIIQ-cfp (cat)*] was created by transforming *Bs168* with genomic DNA from BJW342 [*PY79 refZ::tet, noc::erm, rpoC-gfp (spec), amyE::PspoIIQ-cfp (cat)*] selecting for growth on LB plates containing 7.5 µg/ml chloramphenicol.

BAM118 [*ezrA::kan*] was created by transforming *Bs168* with genomic DNA from BJW438 [*PY79 ezrA::kan*] selecting for growth on LB plates containing 10 µg/ml kanamycin.

BAM125 [*RBM_{5mu}, ezrA::kan*] was created by transforming BJH205 [*RBM_{5mu}*] with genomic DNA from BAM118 [*PY79 ezrA::kan*] selecting for growth on LB plates containing 10 µg/ml kanamycin.

BAM226 [*RBM_{5mu}, sepF::erm*] was created by transforming BJH205 [*RBM_{5mu}*] with genomic DNA from BJH358 [*sepF::erm*] selecting for growth on LB plates containing 1 µg/ml erythromycin (erm) plus 25 µg/ml lincomycin (MLS).

BAM325 [*noc::erm*] was created by transforming *Bs168* with genomic DNA from BJH144 [*PY79 noc::erm*] selecting for growth on LB plates containing 1 µg/ml erythromycin (erm) plus 25 µg/ml lincomycin (MLS).

BAM469 [*Δ(soj-spo0J)::cat, pelB::spo0J (kan)*] was created by transforming BYD029 [*Δ(soj-spo0J)::cat*] with genomic DNA from BYD030 [*pelB::spo0J (kan)*] selecting for growth on LB plates containing 10 µg/ml kanamycin.

BAM908 [RBM_{5mu}*, noc::erm*] was created by transforming BJH205 [RBM_{5mu}] with genomic DNA from BAM325 [*noc::erm*] selecting for growth on LB plates containing 1 µg/ml erythromycin (erm) plus 25 µg/ml lincomycin (MLS).

BAM909 [*amyE::*P_{spoIIG}*-cfp (spec)*] was created by transforming *Bs168* with genomic DNA from BJH369 [*PY79 amyE::*P_{spoIIG}*-cfp (spec)*] selecting for growth on LB plates containing 100 µg/ml spectinomycin.

BAM910 [RBM_{5mu}*, amyE::*P_{spoIIG}*-cfp (spec)*] was created by transforming BJH205 [RBM_{5mu}] with genomic DNA from BJH369 [*PY79 amyE::*P_{spoIIG}*-cfp (spec)*] selecting for growth on LB plates containing 100 µg/ml spectinomycin.

BAM912 [*amyE::*P_{spoIIG}*-cfp (spec), noc::erm*] was created by transforming BAM909 [*amyE::*P_{spoIIG}*-cfp (spec)*] with genomic DNA from BAM325 [*noc::erm*] selecting for growth on LB plates containing 1 µg/ml erythromycin (erm) plus 25 µg/ml lincomycin (MLS).

BAM920 [RBM_{5mu}*, amyE::*P_{spoIIG}*-cfp (spec), noc::erm*] was created by transforming BAM910 [RBM_{5mu}*, amyE::*P_{spoIIG}*-cfp (spec)*] with genomic DNA from BAM325 [*noc::erm*] selecting for growth on LB plates containing 1 µg/ml erythromycin (erm) plus 25 µg/ml lincomycin (MLS).

BAM1265 [*refZ::refZ (WT)(cat)*] was created by transforming BJH247 [*refZ::tet*] with genomic DNA from BAM1006 (3) selecting for growth on LB plates containing 7.5 µg/ml chloramphenicol.

BAM1266 [*refZ::refZ (E53K)(cat)*] was created by transforming BJH247 [*refZ::tet*] with genomic DNA from BAM1024 (3) selecting for growth on LB plates containing 7.5 µg/ml chloramphenicol.

BAM1267 [*refZ::refZ (E61K)(cat)*] was created by transforming BJH247 [*refZ::tet*] with genomic DNA from BAM1026 (3) selecting for growth on LB plates containing 7.5 µg/ml chloramphenicol.

BAM1268 [*refZ::refZ (R102C)(cat)*] was created by transforming BJH247 [*refZ::tet*] with genomic DNA from BAM1012 (3) selecting for growth on LB plates containing 7.5 µg/ml chloramphenicol.

BAM1269 [*refZ::refZ (R102S)(cat)*] was created by transforming BJH247 [*refZ::tet*] with genomic DNA from BAM1014 (3) selecting for growth on LB plates containing 7.5 µg/ml chloramphenicol.

BAM1270 [*refZ::refZ (R116S)(cat)*] was created by transforming BJH247 [*refZ::tet*] with genomic DNA from BAM1020 (3) selecting for growth on LB plates containing 7.5 µg/ml chloramphenicol.

BAM1271 [*refZ::refZ (R116W)(cat)*] was created by transforming BJH247 [*refZ::tet*] with genomic DNA from BAM1018 (3) selecting for growth on LB plates containing 7.5 µg/ml chloramphenicol.

BAM1272 [*refZ::refZ (E117D)(cat)*] was created by transforming BJH247 [*refZ::tet*] with genomic DNA from BAM1022 ((3) selecting for growth on LB plates containing 7.5 µg/ml chloramphenicol.

BAM1273 [*refZ::refZ (E117G)(cat)*] was created by transforming BJH247 [*refZ::tet*] with genomic DNA from BAM1010 (3) selecting for growth on LB plates containing 7.5 µg/ml chloramphenicol.

BAM1274 [*refZ::refZ (L153R)(cat)*] was created by transforming BJH247 [*refZ::tet*] with genomic DNA from BAM1016 (3) for growth on LB plates containing 7.5 µg/ml chloramphenicol.

BAM1275 [*refZ::refZ (E179K)(cat)*] was created by transforming BJH247 [*refZ::tet*] with genomic DNA from BAM1008 (3) selecting for growth on LB plates containing 7.5 µg/ml chloramphenicol.

BAM1280 [*refZ::refZ (WT)(cat), noc::erm*] was created by transforming BAM1265 [*refZ::refZ (WT)(cat)*] with genomic DNA from BAM325 [*noc::erm*] selecting for growth on LB plates containing 1 µg 10 µg/ml erythromycin (erm) plus 25 µg 10 µg/ml lincomycin (MLS).

BAM1281 [*refZ::refZ (E53K)(cat), noc::erm*] was created by transforming BAM1266 [*refZ::refZ (E53K)(cat)*] with genomic DNA from BAM325 [*noc::erm*] selecting for growth on LB plates containing 1 µg/ml erythromycin (erm) plus 25 µg/ml lincomycin (MLS).

BAM1282 [*refZ::refZ (E61K)(cat), noc::erm*] was created by transforming BAM1267 [*refZ::refZ (E61K)(cat)*] with genomic DNA from BAM325 [*noc::erm*] selecting for growth on LB plates containing 1 µg/ml erythromycin (erm) plus 25 µg/ml lincomycin (MLS).

BAM1283 [*refZ::refZ (R102C)(cat), noc::erm*] was created by transforming BAM1268 [*refZ::refZ (R102C)(cat)*] with genomic DNA from BAM325 [*noc::erm*] selecting for growth on LB plates containing 1 µg/ml erythromycin (erm) plus 25 µg/ml lincomycin (MLS).

BAM1284 [*refZ::refZ (R102S)(cat), noc::erm*] was created by transforming BAM1269 [*refZ::refZ (R102S)(cat)*] with genomic DNA from BAM325 [*noc::erm*] selecting for growth on LB plates containing 1 µg/ml erythromycin (erm) plus 25 µg/ml lincomycin (MLS).

BAM1285 [*refZ::refZ (R116S)(cat), noc::erm*] was created by transforming BAM1270 [*refZ::refZ (R116S)(cat)*] with genomic DNA from BAM325 [*noc::erm*] selecting for growth on LB plates containing 1 µg/ml erythromycin (erm) plus 25 µg/ml lincomycin (MLS).

BAM1286 [*refZ::refZ (R116W)(cat), noc::erm*] was created by transforming BAM1271 [*refZ::refZ (R116W)(cat)*] with genomic DNA from BAM325 [*noc::erm*] selecting for growth on LB plates containing 1 µg/ml erythromycin (erm) plus 25 µg/ml lincomycin (MLS).

BAM1287 [*refZ::refZ (E117D)(cat), noc::erm*] was created by transforming BAM1272 [*refZ::refZ (E117D)(cat)*] with genomic DNA from BAM325 [*noc::erm*] selecting for growth on LB plates containing 1 µg/ml erythromycin (erm) plus 25 µg/ml lincomycin (MLS).

BAM1288 [*refZ::refZ (E117G)(cat), noc::erm*] was created by transforming BAM1273 [*refZ::refZ (E117G)(cat)*] with genomic DNA from BAM325 [*noc::erm*] selecting for growth on LB plates containing 1 µg/ml erythromycin (erm) plus 25 µg/ml lincomycin (MLS).

BAM1289 [*refZ::refZ (L153R)(cat), noc::erm*] was created by transforming BAM1274 [*refZ::refZ (L153R)(cat)*] with genomic DNA from BAM325 [*noc::erm*] selecting for growth on LB plates containing 1 µg/ml erythromycin (erm) plus 25 µg/ml lincomycin (MLS).

BAM1290 [*refZ::refZ (E179K)(cat), noc::erm*] was created by transforming BAM1275 [*refZ::refZ (E179K)(cat)*] with genomic DNA from BAM325 [*noc::erm*] selecting for growth on LB plates containing 1 µg/ml erythromycin (erm) plus 25 µg/ml lincomycin (MLS).

BAM1295 [*refZ::cat, noc::erm*] was created by transforming BJH255 [*refZ::cat*] with genomic DNA from BAM325 [*noc::erm*] selecting for growth on LB plates containing 1 µg/ml erythromycin (erm) plus 25 µg/ml lincomycin (MLS).

BAM1296 [*refZ::erm*] was created by transforming *Bs168* with genomic DNA from BKE29630 [*refZ::erm*] (2) selecting for growth on LB plates containing 1 µg/ml erythromycin (erm) plus 25 µg/ml lincomycin (MLS).

BAM1305 [*refZ::refZ (WT)(cat), noc::erm, amyE::P_{cotD}-lacZ (spec)*] was created by transforming BAM1280 [*refZ::refZ (WT)(cat)*] with genomic DNA from BJH323 [*amyE::P_{cotD}-lacZ (spec)*] selecting for growth on LB plates containing 100 µg/ml spectinomycin.

BAM1306 [*refZ::refZ (E53K)(cat), noc::erm, amyE::P_{cotD}-lacZ (spec)*] was created by transforming BAM1281 [*refZ::refZ (E53K)(cat)*] with genomic DNA from BJH323 [*amyE::P_{cotD}-lacZ (spec)*] selecting for growth on LB plates containing 100 µg/ml spectinomycin.

BAM1307 [*refZ::refZ (E61K)(cat), noc::erm, amyE::P_{cotD}-lacZ (spec)*] was created by transforming BAM1282 [*refZ::refZ (E61K)(cat)*] with genomic DNA from BJH323 [*amyE::P_{cotD}-lacZ (spec)*] selecting for growth on LB plates containing 100 µg/ml spectinomycin.

BAM1308 [*refZ::refZ (R102C)(cat), noc::erm, amyE::P_{cotD}-lacZ (spec)*] was created by transforming BAM1283 [*refZ::refZ (R012C)(cat)*] with genomic DNA from BJH323 [*amyE::P_{cotD}-lacZ (spec)*] selecting for growth on LB plates containing 100 µg/ml spectinomycin.

BAM1309 [*refZ::refZ (R102S)(cat), noc::erm, amyE::P_{cotD}-lacZ (spec)*] was created by transforming BAM1284 [*refZ::refZ (R102S)(cat)*] with genomic DNA from BJH323 [*amyE::P_{cotD}-lacZ (spec)*] selecting for growth on LB plates containing 100 µg/ml spectinomycin.

BAM1310 [*refZ::refZ (R116S)(cat), noc::erm, amyE::P_{cotD}-lacZ (spec)*] was created by transforming BAM1285 [*refZ::refZ (R116S)(cat)*] with genomic DNA from BJH323 [*amyE::P_{cotD}-lacZ (spec)*] selecting for growth on LB plates containing 100 µg/ml spectinomycin.

BAM1311 [*refZ::refZ (R116W)(cat), noc::erm, amyE::P_{cotD}-lacZ (spec)*] was created by transforming BAM1286 [*refZ::refZ (R116W)(cat)*] with genomic DNA from BJH323 [*amyE::P_{cotD}-lacZ (spec)*] selecting for growth on LB plates containing 100 µg/ml spectinomycin.

BAM1312 [*refZ::refZ (E117D)(cat), noc::erm, amyE::P_{cotD}-lacZ (spec)*] was created by transforming BAM1287 [*refZ::refZ (E117D)(cat)*] with genomic DNA from BJH323 [*amyE::P_{cotD}-lacZ (spec)*] selecting for growth on LB plates containing 100 µg/ml spectinomycin.

BAM1313 [*refZ::refZ (E117G)(cat), noc::erm, amyE::P_{cotD}-lacZ (spec)*] was created by transforming BAM1288 [*refZ::refZ (E117G)(cat)*] with genomic DNA from BJH323 [*amyE::P_{cotD}-lacZ (spec)*] selecting for growth on LB plates containing 100 µg/ml spectinomycin.

BAM1314 [*refZ::refZ (L153R)(cat), noc::erm, amyE::P_{cotD}-lacZ (spec)*] was created by transforming BAM1289 [*refZ::refZ (L153R)(cat)*] with genomic DNA from BJH323 [*amyE::P_{cotD}-lacZ (spec)*] selecting for growth on LB plates containing 100 µg/ml spectinomycin.

BAM1315 [*refZ::refZ (E179K)(cat), noc::erm, amyE::P_{cotD}-lacZ (spec)*] was created by transforming BAM1290 [*refZ::refZ (E179K)(cat)*] with genomic DNA from BJH323 [*amyE::P_{cotD}-lacZ (spec)*] selecting for growth on LB plates containing 100 µg/ml spectinomycin.

BAM1320 [*refZ::cat, noc::erm, amyE::P_{cotD}-lacZ (spec)*] was created by transforming BAM1295 [*refZ::cat, noc::erm*] with genomic DNA from BJH323 [*amyE::P_{cotD}-lacZ (spec)*] selecting for growth on LB plates containing 100 µg/ml spectinomycin.

BAM1321 [*noc::erm, amyE::P_{cotD}-lacZ (spec)*] was created by transforming BAM325 [*noc::erm*] with genomic DNA from BJH323 [*amyE::P_{cotD}-lacZ (spec)*] selecting for growth on LB plates containing 100 µg/ml spectinomycin.

BAM1322 [*refZ::cat*, *amyE::P_{cotD}-lacZ (spec)*] was created by transforming BJH255 [*refZ::cat*] with genomic DNA from BJH323 [*amyE::P_{cotD}-lacZ (spec)*] selecting for growth on LB plates containing 100 µg/ml spectinomycin.

BAM1323 [*amyE::P_{cotD}-lacZ (spec)*] was created by transforming *Bs168* with genomic DNA from BJH323 [*amyE::P_{cotD}-lacZ (spec)*] selecting for growth on LB plates containing 100 µg/ml spectinomycin.

BAM1324 [*refZ::refZ (WT)(cat)*, *amyE::P_{cotD}-lacZ (spec)*] was created by transforming BAM1265 [*refZ::refZ (WT)(cat)*] with genomic DNA from BJH323 [*amyE::P_{cotD}-lacZ (spec)*] selecting for growth on LB plates containing 100 µg/ml spectinomycin.

BAM1325 [*refZ::refZ (E53K)(cat)*, *amyE::P_{cotD}-lacZ (spec)*] was created by transforming BAM1266 [*refZ::refZ (WT)(cat)*] with genomic DNA from BJH323 [*amyE::P_{cotD}-lacZ (spec)*] selecting for growth on LB plates containing 100 µg/ml spectinomycin.

BAM1326 [*refZ::refZ (E61K)(cat)*, *amyE::P_{cotD}-lacZ (spec)*] was created by transforming BAM1267 [*refZ::refZ (WT)(cat)*] with genomic DNA from BJH323 [*amyE::P_{cotD}-lacZ (spec)*] selecting for growth on LB plates containing 100 µg/ml spectinomycin.

BAM1327 [*refZ::refZ (R102C)(cat)*, *amyE::P$_{cotD}$-lacZ (spec)*] was created by transforming BAM1268 [*refZ::refZ (WT)(cat)*] with genomic DNA from BJH323 [*amyE::P$_{cotD}$-lacZ (spec)*] selecting for growth on LB plates containing 100 µg/ml spectinomycin.

BAM1328 [*refZ::refZ (R102S)(cat)*, *amyE::P$_{cotD}$-lacZ (spec)*] was created by transforming BAM1269 [*refZ::refZ (WT)(cat)*] with genomic DNA from BJH323 [*amyE::P$_{cotD}$-lacZ (spec)*] selecting for growth on LB plates containing 100 µg/ml spectinomycin.

BAM1329 [*refZ::refZ (R116S)(cat)*, *amyE::P$_{cotD}$-lacZ (spec)*] was created by transforming BAM1270 [*refZ::refZ (WT)(cat)*] with genomic DNA from BJH323 [*amyE::P$_{cotD}$-lacZ (spec)*] selecting for growth on LB plates containing 100 µg/ml spectinomycin.

BAM1330 [*refZ::refZ (R116W)(cat)*, *amyE::P$_{cotD}$-lacZ (spec)*] was created by transforming BAM1271 [*refZ::refZ (WT)(cat)*] with genomic DNA from BJH323 [*amyE::P$_{cotD}$-lacZ (spec)*] selecting for growth on LB plates containing 100 µg/ml spectinomycin.

BAM1331 [*refZ::refZ (E117D)(cat)*, *amyE::P$_{cotD}$-lacZ (spec)*] was created by transforming BAM1272 [*refZ::refZ (WT)(cat)*] with genomic DNA from BJH323 [*amyE::P$_{cotD}$-lacZ (spec)*] selecting for growth on LB plates containing 100 µg/ml spectinomycin.

BAM1332 [*refZ::refZ (E117G)(cat)*, *amyE::P$_{cotD}$-lacZ (spec)*] was created by transforming BAM1273 [*refZ::refZ (WT)(cat)*] with genomic DNA from BJH323 [*amyE::P$_{cotD}$-lacZ (spec)*] selecting for growth on LB plates containing 100 µg/ml spectinomycin.

BAM1333 [*refZ::refZ (L153R)(cat)*, *amyE::P$_{cotD}$-lacZ (spec)*] was created by transforming BAM1274 [*refZ::refZ (WT)(cat)*] with genomic DNA from BJH323 [*amyE::P$_{cotD}$-lacZ (spec)*] selecting for growth on LB plates containing 100 µg/ml spectinomycin.

BAM1334 [*refZ::refZ (E179K)(cat)*, *amyE::P$_{cotD}$-lacZ (spec)*] was created by transforming BAM1275 [*refZ::refZ (WT)(cat)*] with genomic DNA from BJH323 [*amyE::P$_{cotD}$-lacZ (spec)*] selecting for growth on LB plates containing 100 µg/ml spectinomycin.

BAM1339 [*ΔrefZ*] was created by transforming BAM1296 [*refZ::erm*] with pDR244 (Cre recombinase plasmid)(2) selecting for growth on LB plates containing 100 µg/ml spectinomycin at 30ºC (permissive). Isolated colonies were propagated on LB plates containing 100 µg/ml spectinomycin at 30ºC, on LB plates at the non-permissive temperature (42ºC), and on LB plates containing MLS (37ºC). Clones were streaked for isolation on LB, spec100, and MLS and a spec and erm sensitive clone was stored.

BAM1359 [*ΔrefZ, noc::erm*] was created by transforming BAM1339 [*ΔrefZ*] with genomic DNA from BAM325 [*noc::erm*] selecting for growth on LB plates containing 1 µg/ml erythromycin (erm) plus 25 µg/ml lincomycin (MLS).

BAM1409 [*ΔrefZ, minD::kan*] was created by transforming BAM1339 [*ΔrefZ*] with genomic DNA from BAM043 [*minD::kan*] selecting for growth on LB plates containing 10 µg/ml kanamycin.

BAM1529 [*ΔrefZ, ezrA::kan*] was created by transforming BAM1339 [*ΔrefZ*] with genomic DNA from BAM118 [*PY79 ezrA::kan*] selecting for growth on LB plates containing 10 µg/ml kanamycin.

BAM1546 [*ΔrefZ, noc::erm, amyE::P_{cotD}-lacZ (spec)*] was created by transforming BAM1359 [*ΔrefZ, noc::erm*] with genomic DNA from BJH323 [*amyE::P_{cotD}-lacZ (spec)*] selecting for growth on LB plates containing 100 µg/ml spectinomycin.

BAM1547 [*RBM_{5mu}, sepF::erm, amyE::P_{cotD}-lacZ (spec)*] was created by transforming BAM226 [*RBM_{5mu}, sepF::erm*] with genomic DNA from BJH323 [*amyE::P_{cotD}-lacZ (spec)*] selecting for growth on LB plates containing 100 µg/ml spectinomycin.

BAM1548 [*sepF::erm, amyE::P_{cotD}-lacZ (spec)*] was created by transforming BJH358 [*sepF::erm*] with genomic DNA from BJH323 [*amyE::P_{cotD}-lacZ (spec)*] selecting for growth on LB plates containing 100 µg/ml spectinomycin.

BAM1549 [*Δ(soj-spo0J)::cat, pelB::spo0J (kan), amyE::P_{cotD}-lacZ (spec)*] was created by transforming BAM469 [*Δ(soj-spo0J)::cat, pelB::spo0J (kan)*] with genomic DNA from BJH323 [*amyE::P_{cotD}-lacZ (spec)*] selecting for growth on LB plates containing 100 µg/ml spectinomycin.

BAM1550 [*ΔrefZ, amyE::P_{cotD}-lacZ (spec)*] was created by transforming BAM1339 [*ΔrefZ*] with genomic DNA from BJH323 [*amyE::P_{cotD}-lacZ (spec)*] selecting for growth on LB plates containing 100 µg/ml spectinomycin.

BAM1557 [*ΔrefZ, sepF::erm*] was created by transforming BAM1339 [*ΔrefZ*] with genomic DNA from BJH358 [*sepF::erm*] selecting for growth on LB plates containing containing 1 µg/ml erythromycin (erm) plus 25 µg/ml lincomycin (MLS).

BAM1559 [*ΔrefZ, ezrA::kan, amyE::P_{cotD}-lacZ (spec)*] was created by transforming BAM1529 [*ΔrefZ, ezrA::kan*] with genomic DNA from BJH323 [*amyE::P_{cotD}-lacZ (spec)*] selecting for growth on LB plates containing 100 µg/ml spectinomycin.

BAM1562 [*RBM_{5mu}, noc::erm, amyE::P_{cotD}-lacZ (spec)*] was created by transforming BAM908 [*RBM_{5mu}, noc::erm*] with genomic DNA from BJH323 [*amyE::P_{cotD}-lacZ (spec)*] selecting for growth on LB plates containing 100 µg/ml spectinomycin.

BAM1563 [*ezrA::kan, amyE::P_{cotD}-lacZ (spec)*] was created by transforming BAM118 [*ezrA::kan*] with genomic DNA from BJH323 [*amyE::P_{cotD}-lacZ (spec)*] selecting for growth on LB plates containing 100 µg/ml spectinomycin.

BAM1564 [*RBM_{5mu}, ezrA::kan, amyE::P_{cotD}-lacZ (spec)*] was created by transforming BAM125 [*RBM_{5mu}, ezrA::kan*] with genomic DNA from BJH323 [*amyE::P_{cotD}-lacZ (spec)*] selecting for growth on LB plates containing 100 µg/ml spectinomycin.

BAM1568 [*ΔrefZ, Δ(soj-spo0J)::cat, pelB::spo0J (kan), amyE::PcotD-lacZ (spec)*] was created by transforming BAM1566 [*ΔrefZ, Δ(soj-spo0J)::cat, pelB::spo0J (kan)*] with genomic DNA from BJH323 [*amyE::P_{cotD}-lacZ (spec)*] selecting for growth on LB plates containing 100 µg/ml spectinomycin.

BAM1569 [*RBM_{5mu}, Δ(soj-spo0J)::cat, pelB::spo0J (kan), amyE::P_{cotD}-lacZ (spec)*] was created by transforming BAM1567 [*RBM_{5mu}, Δ(soj-spo0J)::cat, pelB::spo0J (kan)*] with genomic DNA from

BJH323 [*amyE::P_{cotD}-lacZ (spec)*] selecting for growth on LB plates containing 100 µg/ml spectinomycin.

BAM1573 [*RBM_{5mu}, amyE::P_{cotD}-lacZ (spec)*] was created by transforming BJH205 [*RBM_{5mu}*] with genomic DNA from BJH323 [*amyE::P_{cotD}-lacZ (spec)*] selecting for growth on LB plates containing 100 µg/ml spectinomycin.

BAM1575 [*amyE::P_{cotD}-lacZ (spec), minD::kan*] was created by transforming BAM1323 [*amyE::P_{cotD}-lacZ (spec)*] with genomic DNA from BAM043 [*minD::kan*] selecting for growth on LB plates containing 10 µg/ml kanamycin.

BAM1576 [*RBM_{5mu}, amyE::P_{cotD}-lacZ (spec), minD::kan*] was created by transforming BAM1573 [*RBM_{5mu}, amyE::P_{cotD}-lacZ (spec)*] with genomic DNA from BAM043 [*minD::kan*] selecting for growth on LB plates containing 10 µg/ml kanamycin.

BAM1577 [*ΔrefZ, sepF::erm, amyE::P_{cotD}-lacZ (spec)*] was created by transforming BAM1557 [*ΔrefZ, sepF::erm*] with genomic DNA from BJH323 [*amyE::P_{cotD}-lacZ (spec)*] selecting for growth on LB plates containing 100 µg/ml spectinomycin.

BAM1578 [*ΔrefZ, minD::kan, amyE::P_{cotD}-lacZ (spec)*] was created by transforming BAM1409 [*ΔrefZ, minD::kan*] with genomic DNA from BJH323 [*amyE::P_{cotD}-lacZ (spec)*] selecting for growth on LB plates containing 100 µg/ml spectinomycin.

BAM1600 [*refZ::tet, amyE::P_{spoIIQ}-cfp (cat)*] was created by transforming BJH247 [*refZ::tet*] with genomic DNA from BAM067 [*amyE::P_{spoIIQ}-cfp (cat)*] selecting for growth on LB plates containing 7.5 µg/ml chloramphenicol.

BAM1601 [*RBM_{5mu}, amyE::$_{PspoIIQ}$-cfp (cat)*] was created by transforming BJH205 [*RBM_{5mu}*] with genomic DNA from BAM067 [*amyE::P_{spoIIQ}-cfp (cat)*] selecting for growth on LB plates containing 7.5 µg/ml chloramphenicol.

BAM1603 [*amyE::P_{spoIIG}-cfp (spec), refZ::tet*] was created by transforming BAM909 [*amyE::P_{spoIIG}-cfp (spec)*] with genomic DNA from BJH247 [*refZ::tet*] selecting for growth on LB plates containing 10 µg/ml tetracycline.

BAM1604 [*amyE::P_{spoIIG}-cfp (spec), noc::erm, refZ::tet*] was created by transforming BAM912 [*amyE::P_{spoIIG}-cfp (spec), noc::erm*] with genomic DNA from BJH247 [*refZ::tet*] selecting for growth on LB plates containing 10 µg/ml tetracycline.

BAM1610 [*refZ::tet, amyE::P_{spoIIQ}-cfp (cat), noc::erm*] was created by transforming BAM1600 [*refZ::tet, amyE::P_{spoIIQ}-cfp (cat)*] with genomic DNA from BAM325 [*noc::erm*] selecting for growth at 30ºC on LB plates containing 1 µg/ml erythromycin (erm) plus 25 µg/ml lincomycin (MLS).

BAM1611 [*RBM_{5mu}, amyE::$_{PspoIIQ}$-cfp (cat), noc::erm*] was created by transforming BAM1601 [*RBM_{5mu}, amyE::$_{PspoIIQ}$-cfp (cat)*] with genomic DNA from BAM325 [*noc::erm*] selecting for growth at 30ºC on LB plates containing 1 µg/ml erythromycin (erm) plus 25 µg/ml lincomycin (MLS).

BAM1638 [*amyE::P_{spoIIQ}-cfp (cat), rpoC-gfp (spec)*] was created by transforming BAM067 [*amyE::P_{spoIIQ}-cfp (cat)*] with genomic DNA from BJW342 [*PY79 refZ::tet, noc::erm, rpoC-gfp (spec), amyE::PspoIIQ-cfp (cat)*] selecting for growth at 30ºC on LB plates containing 100 µg/ml spectinomycin.

BAM1639 [*refZ::tet, amyE::P_{spoIIQ}-cfp (cat), noc::erm, rpoC-gfp (spec)*] was created by transforming BAM1610 [*refZ::tet, amyE::P_{spoIIG}-cfp (spec), noc::erm*] with genomic DNA from BJW342 [*PY79 refZ::tet, noc::erm, rpoC-gfp (spec), amyE::P_{spoIIQ}-cfp (cat)*] selecting for growth at 30ºC on LB plates containing 100 µg/ml spectinomycin.

BAM1640 [*RBM_{5mu}, amyE::$_{PspoIIQ}$-cfp (cat), noc::erm, rpoC-gfp (spec)*] was created by transforming BAM1611 [*RBM_{5mu}, amyE::P_{spoIIG}-cfp (spec), noc::erm*] with genomic DNA from BJW342 [*PY79 refZ::tet, noc::erm, rpoC-gfp (spec), amyE::P_{spoIIQ}-cfp (cat)*] selecting for growth at 30ºC on LB plates containing 100 µg/ml spectinomycin.

References

1. **Miller AK, Brown EE, Mercado BT, Herman JK.** 2016. A DNA-binding protein defines the precise region of chromosome capture during *Bacillus* sporulation. Mol Microbiol **99:**111-122.
2. **Koo BM, Kritikos G, Farelli JD, Todor H, Tong K, Kimsey H, Wapinski I, Galardini M, Cabal A, Peters JM, Hachmann AB, Rudner DZ, Allen KN, Typas A, Gross CA.** 2017. Construction and Analysis of Two Genome-Scale Deletion Libraries for *Bacillus subtilis*. Cell Syst **4:**291-305 e297.
3. **Brown EE, Miller AK, Krieger IV, Otto RM, Sacchettini JC, Herman JK.** 2019. A DNA-Binding Protein Tunes Septum Placement during *Bacillus subtilis* Sporulation. J Bacteriol **201**.